LAWRENCE
LIVERMORE
NATIONAL
LABORATORY

LLNL-JRNL-522612

Old-Growth CO2 Measurements Reveal High Sensitivity to Climate Anomalies across Seasonal, Annual and Decadal time scales

S. Wharton, M. Falk, K. Bible, M. Schroeder, K. T. Paw U

January 10, 2012

Agricultural and Forest Meteorology

Disclaimer

Old-growth CO_2 measurements reveal high sensitivity to climate anomalies across seasonal, annual and decadal time scales

Wharton, S.[1,*], Falk, M.[2], Bible, K.[3], Schroeder, M.[3], Paw U, K.T.[2]

[1]Atmospheric, Earth and Energy Division, Lawrence Livermore National Laboratory, Livermore, California

[2]Dept. Land, Air and Water Resources, University of California, Davis, California,

[3]College of the Environment, University of Washington, Seattle, Washington

*Corresponding author: wharton4@llnl.gov, voice 925-422-9295, fax 925-422-5844

Keywords: FLUXNET, net ecosystem exchange, CO2 flux, teleconnections, PDO, ENSO, interannual variability, long-term fluxes

Abstract

The traditional hypothesis that old-growth forests are carbon neutral is under debate as recent studies show evidence of net carbon sequestration. Here, we present a decade (1998-2008) of carbon dioxide, water and energy fluxes from an old-growth stand in the American Pacific Northwest to identify ecosystem-level responses to climate variability, including teleconnection patterns. This study provides the longest, continuous record of old-growth eddy flux data to date. From 1998-2008, average annual net ecosystem exchange (F_{NEE}) was - 49 ± 40 g C m^{-2} yr^{-1} (a small net carbon sink) while interannual variability was high (~ 300 g C m^{-2} yr^{-1}) and indicated that the stand is able to switch from net carbon sink to source in response to climate forcing. Seasonal and annual F_{NEE} variability was strongly linked to climate anomalies associated with major teleconnections and the subsequent responses of driving mechanisms (e.g., water use efficiency, light use efficiency, canopy conductance) to local weather (e.g., cloudiness). Biometric measurements of aboveground net primary productivity (F_{ANPP}) provided a ~60 year record of growth, recruitment, and mortality responses to a longer range of climatic conditions, including shifts in the Pacific Decadal Oscillation (PDO). A negative trend in F_{ANPP} generally matched the warm PDO phase shift starting in 1977. As climate models predict future warming in the Pacific Northwest, our results suggest that any perturbations towards a warmer, drier state, such as would occur during positive climate phases, may have significant impacts on regional terrestrial carbon budgets through increasing respiration without subsequent, offset increases in carbon assimilation in these old-growth forests.

1.1 Introduction

Fluxes of energy, water, and carbon at forest ecosystems have been extensively studied with the eddy covariance (EC) technique over the last couple of decades. At present, over 150 FLUXNET sites have long enough (ten years or more) records to examine the influence on interannual climate variability on net ecosystem exchange of carbon (F_{NEE}). Some of the longest, continuous data records for forest sites include: Harvard forest, Massachusetts, USA since 1991 (Goulden et al. 1996, Urbanski et al. 2007); Takayama, Japan (Saigusa et al. 2002) since 1993; BOREAS NSA-Old Black Spruce, Manitoba, Canada (Dunn et al. 2007), BOREAS SSA-Old Black Spruce, Saskatchewan, Canada (Amiro et al. 2006, Bergeron et al. 2007) and SSA-Old Jack Pine, Saskatchewan, Canada (Amiro et al. 2006) since 1994; Camp Borden, Ontario, Canada (Lee et al. 1999, Barr et al. 2002), Loobos, The Netherlands (Dolman et al. 2002, Gusev et al. 2005) and Howland, Maine, USA (Hollinger et al. 1999, 2004) since 1995; Brasschaat, Belgium (Janssens et al. 2001, Carrara et al. 2003), Vielsalm, Belgium (Valentini et al. 2000, Aubinet et al. 2001), SSA-Old Aspen, Saskatchewan, Canada (Amiro et al. 2006, Barr et al. 2007), Sorø-LilleBogeskov, Denmark (Pilegaard et al. 2001), Hyytiälä, Finland (Markkanen et al. 2001, Kolari et al 2009), Hesse Forest, France (Granier et al. 2000), Tharandt-Anchor Station, Germany (Grunwald 2003), Castelporziano, Italy (Valentini et al. 2000, Reichstein et al. 2003), Flakaliden, Sweden (Lindroth et al. 1998), and Norunda, Sweden (Lindroth et al. 1998) since 1996 (http://www.fluxnet.ornl.gov/fluxnet/viewstatus.cfm).

Many of these EC studies have focused on the role of climate variability on interannual F_{NEE} although capturing the true range of flux response to climate anomalies has often been hampered by concurrent biological changes or disturbances in the ecosystem or by the lack of strong climate fluctuations during the measurement record. For example, year-to-year changes

70 in F_{NEE} at some forests appear to be partially linked to structural changes (Urbanski et al. 2007)
71 or to variations in biotic responses (Richardson et al. 2007) in addition to changes in climate.
72 Forest stand properties such as biomass growth, successional changes, or increases in mortality
73 may change over relatively short time scales after a natural disturbance or from altered
74 management practices. These factors make it difficult to isolate the effects of climate variability
75 on F_{NEE} at many sites. For example, year-to-year changes in annual F_{NEE} at a ~100 year old
76 mixed deciduous forest were uncorrelated to environmental drivers, and instead, linked to
77 increases in tree biomass, successional changes in forest species composition, and disturbance,
78 while short term (from hours to months) CO_2 flux perturbations appeared to be caused by the
79 changing environment (e.g., warmer temperatures or increased light levels) (Urbanski et al.
80 2007).
81 EC measurements are regularly taken over stands of managed, even-aged forests of less
82 than 100 years old (e.g., Arain & Restrepo-Coupe 2005, Markkanen et al. 2001, Morgenstern et
83 al. 2004) while less is known about the seasonal dynamics and interannual variability of fluxes in
84 a complex, old-growth forest ecosystem such as the one investigated here. Pacific Northwest
85 old-growth Douglas-fir forests, including our site, have large, live old trees (175–350+ years
86 old), tall canopy height (> 50 m), large snags, and large logs on the ground (Franklin et al. 1981;
87 Franklin & Spies 1991). These old-growth stands once covered large parts of the Pacific
88 Northwest before the onset of industrial timber operations. Today, they represent a small
89 fraction of western North America: in Oregon and Washington about 10% (1.1 million hectares)
90 of the original old-growth forests remain (Franklin & Spies 1991). While these old-growth
91 forests are small in land coverage, they represent a significant pool of carbon that has been stored

92 for centuries in the soil, aboveground biomass, and woody debris that could be released into the
93 atmosphere after a disturbance, such as clear-cut harvesting or one induced by climate change.
94 It had been assumed that mortality balances growth in old-growth forests making them
95 carbon neutral (Odum, 1965, Franklin et al. 1981), although a number of EC (Hollinger et al.
96 1994, Anthoni et al. 2002, Griffis et al. 2003, Knohl et al. 2003, Loescher et al. 2003, Desai et al.
97 2005, Tan et al. 2011) and recent forest inventory (Hudiburg et al. 2009, Lichstein et al. 2009)
98 studies in mature and old-growth stands are showing that the late seral class may in fact be a
99 significant net sink of atmospheric CO_2. From studying a combination of EC fluxes, biometric,
100 and modeled data, Luyssaert et al. (2008) suggest that forests older than 200 years old sequester
101 on average 240 ± 80 g C m^{-2} yr^{-1}, with half of that amount stored belowground in the roots and
102 soil organic matter. Furthermore, old-growth forests may have the potential to sequester carbon
103 at higher rates (> 300 g C m^{-2} yr^{-1}) similar to younger forests if climatic conditions are favorable.
104 This behavior has been observed at La Selva, an old-growth forest in Costa Rica. During
105 relatively wet and cool dry seasons in La Niña years the tropical forest sequestered 310-792 g C
106 m^{-2} yr^{-1} (Loescher et al. 2003).
107 Biometric measurements from old-growth trees have also shown climate-related
108 variability. Tree ring measurements taken from a Manitoba, Canada old-growth spruce forest
109 indicated a periodicity of approximately 7 years and suggest a link between tree growth and
110 oscillating environmental factors while variation in ring width could not be linked directly to
111 annual changes in temperature and precipitation (Rocha et al. 2006). Such multi-year
112 measurements from Loescher et al. and Rocha et al. illustrate the significance of weather
113 anomalies associated with climate periodicities (i.e., teleconnection patterns). In the western
114 Americas, climate is influenced by major Pacific ocean-atmospheric oscillations. These include

115 the 40-50 day Madden and Julian Oscillation (Madden & Julian 1971), 2-7 year El Nino-
116 Southern Oscillation (Rasmusson & Wallace 1983), 10 year Pacific/North American Oscillation
117 (Wallace & Gutzler 1981), and 20-30 year Pacific Decadal Oscillation (Mantua & Hare 2002).
118 Here, we present a decade (1998-2008) of carbon dioxide, water and energy fluxes from a
119 low elevation, old-growth forest with no recent major disturbances, biomass, or structural
120 changes that has been exposed to a wide spectrum of climate variability including recent phase
121 shifts of the PDO, ENSO and PNA. In addition, biometric data provided an independent, long-
122 term (1947-2004) measurement record of growth, recruitment, and mortality responses to a
123 longer range of climatic conditions including the 1977 major PDO phase change. Our objectives
124 were to: (1) test the traditional ecological hypothesis that an old-growth forest is an insignificant
125 net annual carbon sink and is carbon neutral, (2) investigate the response of old-growth carbon
126 exchange to changing environmental and climatic factors across seasonal, annual and decadal
127 time scales by utilizing eddy covariance and biometric forest inventory data, and (3) identify the
128 mechanistic drivers of interannual CO_2 flux variability.
129
130 **1.2 Site Description**
131 The Wind River Field Station (formerly the Wind River Canopy Crane Research Facility)
132 is located in a 500-hectare old-growth, evergreen needleleaf forest in the T.T. Munger Research
133 Natural Area (RNA), a protected section of the Gifford Pinchot National Forest in southern
134 Washington State, USA (45° 49' 13.76" N; 121° 57' 06.88" W, 371 m above sea level). The
135 stand has never been managed and is thought to have originated after a natural fire around the
136 year 1500. Stand characteristics are briefly given here while Shaw et al. (2004) provide a
137 detailed ecological description. Unique stand properties include large standing biomass and

large amounts of coarse woody debris on the forest floor. Total estimated biomass is 619 Mg C ha^{-1}, of which 398 Mg C ha^{-1} is stored in live biomass and 221 Mg C ha^{-1} in soil and coarse and fine woody debris (Harmon et al. 2004). Maximum rooting depth is 1-2 m for the tallest, dominant Douglas-fir trees although most of the root biomass is concentrated in the first 0.5 m. The water table depth is seasonally variable and ranges from 0.3 to 0.5 m in the wet winter months to a depth of 2.0-2.4 m in the summer and early autumn.

The old-growth forest is dominated by evergreen conifer species. Douglas-fir (*Pseudotsuga menziesii* (Mirbel) Franco) represent the largest trees in diameter and height, while western hemlock (*Tsuga heterophylla* (Raf.) Sarg), a shade-tolerant species, will eventually outnumber all other species in the stand. Average tree heights are 52 m for Douglas-fir and 19 m for western hemlock (Ishii et al. 2000). Deciduous vegetation is not a significant component of stand biomass comprising no more than 15% of canopy structure during the summer months (Thomas & Winner 2000). Stand density is approximately 427 trees per hectare, tree ages range from 0 to ~500 years (Shaw et al. 2004), and leaf area index (LAI) measurements range from 8.2 to 9.2 m^2 m^{-2} with little seasonality (Thomas & Winner 2000, Roberts et al. 2004, Parker et al. 2002).

1.3 Climate

The climate is characterized by wet and mild winters interspersed with a strong, seasonal summer drought (Shaw et al. 2004, Falk et al. 2005). Meteorological records are available from the nearby USFS Wind River Ranger Station (1919-1977) (45º 28' 47" N, 121º 33' 36" W, 351.1 m a.s.l) and Carson Fish Hatchery NOAA weather station (1977-2008) (45º 31' 12" N, 121º 34' 48" W, 345.6 m a.s.l). Historical mean annual air temperature is 8.8 ^{o}C and total water-year

precipitation is 2338 mm, of which on average only 322 mm falls from July through October. Due to strong seasonality, total precipitation is defined here by water-year (November-October) instead of annually (January-December).

Regional interannual and decadal climate variability is driven by the presence and magnitude of interrelated equatorial and extratropical ocean-atmospheric oscillations, including the Pacific Decadal Oscillation (PDO), Pacific/North American Oscillation (PNA), and El Niño-Southern Oscillation (ENSO) (Mote et al. 2003). Positive phases of the PDO index, PNA index, and Multivariate ENSO index (MEI) bring significantly warmer and drier winters to Wind River while negative phases bring cooler and wetter conditions (Wharton et al. 2009). To take advantage of in-phase additive teleconnection patterns, a single climate index, the Composite Climate Index (CCI), was developed by Wharton et al. (2009). In brief, CCI is calculated from the sum of autumn-winter-spring PDO, PNA, and MEI magnitudes. Years with CCI values below -1.0 are classified as negative or cool phase years, years with CCI values above +1.0 are positive or warm phase years, and years with CCI values between -1.0 and +1.0 are neutral phase years. The CCI intrinsically contains information about cloudiness, temperature, vapor pressure deficit, light levels, and moisture as the Pacific Oscillation Indices are calculated from large-scale perturbations in atmospheric pressure (PNA and MEI), sea surface temperature (PDO and MEI), surface wind (MEI), air temperature (MEI), and cloudiness (MEI).

2. Materials and Methods

2.1 Biometric data

The T.T. Munger RNA has 40 ha of permanent plots in nine parallel belt transects. These plots were established in 1947 and are remeasured approximately every six years to gather data

184 on tree recruitment, growth, and mortality. The last remeasurement was done in 2004. Average
185 Aboveground Net Primary Productivity (F_{ANPP}) (g C m^{-2} y^{-1}) was calculated as the mean change
186 in live tree carbon storage plus tree mortality and recruitment over the remeasurement interval
187 following methods in Harmon et al. (2004). In contrast to the eddy flux measurements, F_{ANPP}
188 does not include heterotrophic respiration fluxes, belowground autotrophic respiration, or
189 belowground carbon storage (e.g., changes in root biomass).
190
191 **2.2 Micrometeorological data**
192 Site specific micrometeorological measurements were collected as 30-minute averages
193 from July 1998 through December 2008 at the Wind River AmeriFlux tower. Radiation
194 measurements included above canopy (70m) incoming photosynthetic photon flux density (Q_p)
195 (µmol quantum m^{-2} s^{-1}) (190SB, LI-COR, Lincoln, Nebraska, USA) and below canopy (2m) Q_p.
196 Air temperature (T_a) (ºC) and relative humidity (RH) (%) (HMP-35C, Vaisala, Inc., Oy, Finland)
197 were measured at 2 m and 70 m. Soil temperature (T_s) (ºC) was measured at depths of 0.05, 0.15
198 and 0.30 m (CS106B, Campbell Scientific Inc., Logan, Utah, USA).
199 Measurements of water availability included precipitation (P) (mm) and volumetric soil
200 moisture (θ_v) (m^3 m^{-3}). θ_v was measured at depths from 0.2 m to 2 m (4 replicates) using soil
201 moisture probes (EnviroSMART, Sentek Sensor Technologies, Stepney, Australia). Precipitation
202 was measured using a rain and snow gauge 5 km away at the Carson Fish Hatchery at a similar
203 elevation as the site.
204 The Standardized Precipitation Index (SPI) was calculated to compare precipitation
205 amounts during the flux years to the long-term meteorological record (1919-1997) following
206 McKee et al. (1993). Positive SPI values indicate above normal precipitation while negative SPI

values indicate below normal. By definition, the SPI ranges from -3 (extremely dry) to +3 (extremely wet). A drought event is defined when the SPI is continuously negative at a value of -1 or less over the time scale of interest. We calculated two standard precipitation indices: a 6-month SPI to identify longer-term precipitation anomalies that may reflect anomalies in soil reservoir storage and a 3-month SPI to determine shorter drought features.

2.3 Ecosystem CO_2, H_2O, and energy fluxes

Half-hour fluxes of carbon dioxide (F_c) (μmol m^{-2} s^{-1}), water vapor (F_{H2O}) (mmol m^{-2} s^{-1}), latent energy (λE) (W m^{-2}), and sensible heat (H) (W m^{-2}) were measured continuously with the EC method since July 1998 at the tower. The system consisted of a 3-dimensional sonic anemometer/thermometer (HS-100 until March 2009, GILL Instruments, Lymington, UK; CSAT3 after March 2009, Campbell Scientific Inc.) and a closed path infrared gas analyzer (IRGA) (LI-6262 until February 2006; LI-7000 after February 2006, LI-COR). The EC system is located above the canopy at a height of 68.4 meters above ground.

10 Hz wind data were rotated to align the streamwise velocity (u) with the mean wind direction and corrected for lateral momentum transfer (Schotanus et al. 1983), high frequency loss (Moore 1986, Leuning & Judd 1996), and sensor separation between the sonic anemometer and IRGA air inlet (Moore 1986, Massman & Lee 2002). Footprint modeling following Wilson & Swaters (1991) indicated that fetch was good in all directions during strongly convective atmospheric conditions, but inadequate under strongly stable conditions. For the remaining stability regimes, footprint homogeneity was sensitive to wind direction and source fluxes originating from northeast-to-southeast wind sectors were removed due to heterogeneous (age fragmented) land cover.

Following Falk et al. (2005, 2008), half-hour net ecosystem exchange fluxes (F_{NEE}) ($\mu mol\ m^{-2}\ s^{-1}$) were calculated to include storage CO_2 fluxes (F_s) as well as the direct EC measurement (F_c):

$$F_{NEE} = F_c + F_s \quad (1)$$

2.4 Data exclusion criteria for eddy fluxes

The CO_2 and H_2O fluxes were averaged over 30-minutes and flagged if the data met any one of the following criteria: (1) an incomplete half-hour, (2) instrument failure, (3) wind direction from 45-135 degrees, (4) major rain or snow, or (5) significant flux outliers (magnitudes above or below the 95% confidence interval). Flagged data were removed and gap-filled using techniques described in Section 2.6. Percentage of flagged data ranged from 14% in 2002 to 71% in 2005. High data losses in 1998 and 2005 were due to instrument failure. In addition, nighttime CO_2 fluxes were screened to ensure that they were measured during adequate turbulence conditions using the methodology described in Section 2.5. Nighttime turbulence screening resulted in an additional 55% (2006) to 77% (2003) of nocturnal data requiring correction.

2.5 Nighttime F_c corrections and F_{Reco}

A stable atmosphere, which commonly occurs at night, causes the suppression of turbulence leading to laminar flow regimes, intermittent turbulence, or the presence of gravity waves. During these conditions, the theoretical assumptions of eddy-covariance are violated and measurements of mass and energy exchange are problematic. Nighttime CO_2 fluxes must be "corrected" in order to calculate defensible sums of annual F_{NEE}. We used the ustar (u_*)

253 correction method to replace nighttime F_c during periods of inadequate turbulence in
254 combination with a respiration model based on air temperature and soil moisture. Half-hour,
255 nighttime F_c were included in the respiration model if all of the following criteria were met: (1)
256 incoming shortwave radiation < 1 W m^{-2}, (2) $u_* > 0.3$ m s^{-1} (called the u_* critical threshold), (3)
257 $F_c > -25$ μmol m^{-2} s^{-1} or $F_c < 35$ μmol m^{-2} s^{-1} (negative fluxes were kept so not to artificially bias
258 the dataset towards positive only values), and (4) F_c flux was in the 95% confidence interval.
259 The half-hour carbon dioxide fluxes were then binned into 0.5 ºC temperature classes and fitted
260 with exponential temperature and moisture attenuation functions (see Falk et al. 2005, 2008 for
261 further details).
262
263 **2.6 Gap filling methods**
264 We implemented two gap filling strategies, which vary in degrees of sophistication, to
265 model half-hour F_{NEE}. Following the mean diurnal variation method described in Falge et al.
266 (2001), our first gap filling method used a FORTRAN90 code with a fixed 14 day time window
267 to fill any missing or flagged F_{NEE} half-hours. This method is able to reproduce non-linearity
268 ecosystem responses due to diurnal changes, but can also introduce errors during short-term gap
269 filling periods when unusual weather conditions arise and the appropriate corresponding plant
270 functional responses are not well represented by the mean diurnal fluxes.
271 Our second method, following Reichstein el al. (2005), used both a temporal auto-
272 correlation of fluxes with a time window of ± 7 days and the covariance of fluxes with
273 meteorological variables, i.e. “look-up” tables (http://gaia.agraria.unitus.it/database/eddyproc/).
274 Instrument failure and subsequent large data gaps in 1998 and 2005 caused these years to be gap-

275 filled additionally with the process-based ecosystem model Biome-BGC (v4.1.2) (Thornton et al.
276 2002). Ecophysiological parameter values for Wind River were based on Thornton et al. (2002).
277
278 **2.7 Daily, monthly, and annual F_{NEE}, F_{Reco}, and F_{GPP}**
279 Partitioning F_{NEE} into the larger component fluxes respiration (F_{Reco}) and photosynthesis
280 (or gross primary production, F_{GPP}) is essential for understanding the drivers of seasonal and
281 interannual F_{NEE} variability (Baldocchi 2008). Daily integrated F_{NEE} and F_{Reco} were used to
282 estimate F_{GPP} (g C m^{-2} day^{-1}):
283 $$F_{GPP} = F_{NEE} - F_{Reco} \quad (2)$$
284 F_{Reco} and F_{GPP} are always assigned positive values such that if F_{NEE} is negative, carbon uptake by
285 photosynthesis is greater than carbon loss by ecosystem respiration. Monthly and annual fluxes
286 were calculated from daily sums.
287 We estimated uncertainty in annual F_{NEE} using the bootstrapping technique with the
288 Monte Carlo approach following methodology in Ma et al. (2007). Here, uncertainties in annual
289 F_{NEE} were based on the 95% confidence interval from running 5000 simulations of daily F_{NEE}.
290
291 **2.8 Bulk canopy and efficiency parameters: G_c, WUE, LUE**
292 Canopy conductance (G_c) (m s^{-1}), light use efficiency (LUE) (g C MJ^{-1}), and water use
293 efficiency (WUE) (g C kg^{-1} H_20) were derived using a combination of micrometeorological and
294 EC data to investigate mechanistic responses to weather and climate anomalies. Following
295 Stewart (1988), G_c was estimated using the inverted Penman-Monteith equation (Monteith
296 1964):

297 $$G_c = \left[\frac{\rho c_p \delta e}{\gamma \lambda E} + \frac{\frac{\Delta}{\gamma}\beta - 1}{G_a} \right]^{-1} \quad (3)$$

298 where ρ is air density (kg m^{-3}), c_p is specific heat (J kg^{-1} K^{-1}), δe is vapor pressure deficit (kPa), γ
299 is the psychrometric constant (kPa K^{-1}), Δ is slope of the saturation vapor pressure curve (kPa K^{-1}),
300 β is Bowen ratio ($\frac{H}{\lambda E}$), and G_a is aerodynamic conductance for momentum transfer (G_a =
301 $\frac{u_*^2}{U}$) (m s^{-1}).

302 LUE describes how efficient plants are at using light for carbon assimilation (Monteith
303 1972, 1977) and was calculated based on the mass of carbon assimilated (g C) for every
304 megajoule (MJ) of light intercepted by the canopy ($Q_{p,i}$):

305 $$LUE = F_{GPP} / Q_{p,i} \quad (4)$$

306 Where $Q_{p,i}$ (MJ m^{-2} day^{-1}) was calculated using above canopy Q_p, LAI, and a varying light
307 extinction coefficient (see Wharton et al. 2009).

308 Because diffuse radiation measurements were not available, we were unable to identify
309 any ecophysiological response differences to direct versus diffuse radiation. Instead, we
310 categorized daily incoming Q_p data into dark and cloudy, cloudy, partly cloudy, and sunny
311 periods based on a clear sky fraction (CSF):

312 $$CSF = Q_p / Q_{pmax} \quad (5)$$

313 CSF by definition ranges from 0 (minimum brightness, cloudy sky) to 1 (maximum brightness,
314 clear sky). The advantage of CSF is that it implicitly provides information about wavelength,
315 intensity, and scattering of light as well as temperature, moisture, and vapor pressure deficit.
316 WUE is defined as the total mass of dry matter (g C) produced by photosynthesis for
317 every kilogram of water lost by vegetation through transpiration (Rosenberg et al. 1983).
318 Continuous measurements of transpiration (e.g., from sap-flow measurements) were not
319 available. Therefore, WUE was modified to represent the total mass of carbon assimilated for
320 every gram of water lost by the ecosystem through evapotranspiration (E_T):

321 $$WUE = F_{GPP} / E_T \quad (6)$$

322

323 **3. Results**

324 **3.1 Climate variability**

325 *3.1.1 Seasonal and annual trends*

326 Climate seasonality is historically strong at Wind River: on average more than 60% of
327 water-year precipitation falls between November-March, 25% between April-June, and less than
328 15% between July-October. The dry season usually begins in late June to early July and ends in
329 late September to mid-October. During the flux period (1998-2008), conditions were generally
330 warmer and drier than the historical (1919-1997) mean (8.8 ^{o}C, 2338 mm water-year^{-1}). From
331 1998-2008, mean annual air temperature was 9.0 ^{o}C and total water-year precipitation was 2142
332 mm.

333 Interannual and interseasonal climate variability was large during the flux period (Figure
334 1). Annual mean air temperature varied from 8.09 ^{o}C in 2008 to 9.75 ^{o}C in 1998. 1998, 2003,

and 2004 were more than 0.70 ^{o}C warmer than the historical average. In addition, these years were in the upper 90th percentile for mean minimum temperature. Total water-year precipitation varied by more than 1500 mm and ranged from 1334 mm in 2000-2001 to 2878 mm in 1998-1999. 2000-2001 had the lowest measurable precipitation since records began in 1919, while 1998-1999 was in the upper 20th percentile of historically wettest years. Below normal water-years were mostly due to dry March-June conditions although unusually dry winters were also observed in 2001 and 2005. Dry season (July-October) precipitation was below the historical mean (322 mm) during all flux years except 2004 (492 mm).

3.1.2 Influence of teleconnections

Negative CCI phase years included 1999, 2000, and 2008, positive CCI years included 1998, 2003, and 2005, and 2001, 2002, 2004, 2006, and 2007 were classified as neutral. Positive CCI years were on average warmer and drier than normal and include the strong El Niño event of 1998, moderate El Niños in 2003 and 2005, and warm, winter-time phases of the PDO and PNA. Negative CCI years were on average cooler and wetter and include in-phase La Niña, cool PDO and cool PNA events (Table 1 and Figure 1).

3.1.3 Standardized Precipitation Index and summer drought

Significant anomalies in the 6-month SPI occurred during the rainy season (November-April) in 1999 (moderately wet, SPI = +1.4), 2001 (extremely dry, - 2.9), 2005 (severely dry, - 1.9) and growing season (March-August) in 2006 (moderately dry, - 1.3) and 2007 (extremely dry, - 2.5) (Figure 2). A long-term drought event lasted from November 2000-July 2001 and the 6-month SPI averaged -2.1. The 3-month SPI indicated significant precipitation anomalies in

June-August 1998 (moderately dry, - 1.5), March-May 2001 (severely dry, -1.6), July-September 2002 (severely dry, - 1.9a), July-September 2003 (extremely dry, - 2.2), April-June 2007 (extremely dry, -2.5), as well as very wet conditions in June-August 2004 (+ 1.7). Short-term drought events occurred at the end of summer/early autumn in 2002, 2003 and 2006, and during early summer in 2007.

The average summer dry season resulted in very low soil moisture with values as low as 10-15% in the upper 20 cm of the soil in August and September before rains returned in early autumn. In 2002 and 2006, very dry near-surface θ_v (<15%) conditions extended into October. The deeper soil layers, for comparison, were wetter throughout the dry season: the 50 cm soil layer (within reach of most of the coarse root biomass) was generally 10% wetter than the near-surface, while the 150 cm depth (within reach of the tallest, dominant Douglas-fir trees) was 15-20% wetter than near-surface conditions.

3.2 Seasonal patterns in F_{NEE}, F_{GPP}, F_{Reco}

Maximum monthly carbon uptake occurred in April in all years except for 2000, 2004 and 2005 (May) (Table 2) and averaged -71 g C m^{-2} mo^{-1}. On average, net sink months included February through June while all other months were a small to moderate net carbon source (up to + 22 g C m^{-2} mo^{-1} in July). F_{GPP} on average peaked in May while F_{Reco} showed a clear seasonal pattern with temperature and peaked in July. Average key seasonal carbon flux transitions at Wind River include:

(1) The transition from winter with low light levels (Q_p < 60 MJ m^{-2} mo^{-1}), saturated soil conditions (θ_v > 0.3 m^3 m^{-3}), low air temperatures (T_{air} < 5°C), and low vapor pressure deficit (maximum daily δe < 0.3 kPa) to spring with the highest rates of daily F_{NEE} under cool (5 < T_a < 15 °C), wet (θ_v > 0.25 m^3 m^{-3}), adequate light (100 < Q_p < 200 MJ m^{-2} mo^{-}

382 ^{1}), and low-to-moderate δe (< 1.5 kPa) conditions. Springtime conditions favor
383 photosynthesis and the greatest difference between daily F_{GPP} (larger flux) and F_{Reco}
384 (smaller flux) is observed in April-May.
385
386 (2) The end of the cool, rainy season in June and start of the warm, dry season with air
387 temperatures above 15 ^{o}C, low soil moisture ($\theta_v < 0.25$ m^3 m^{-3}), high light levels ($Q_p >$
388 200 MJ m^{-2} mo^{-1}), and high vapor pressure deficit (maximum daily $\delta e > 1.5$ kPa). The
389 old-growth forest transitions to a net carbon source due to reduced photosynthesis caused
390 by low water availability (low precipitation, low θ_v) and high water demand (high δe) and
391 enhanced respiration due to higher temperatures.
392
393 (3) The end of drought in September-October when rains return and maximum air
394 temperatures drop below 15 ^{o}C, vapor pressure deficit decreases ($\delta e < 1$ kPa), soil
395 moisture increases ($\theta_v > 0.25$ m^3 m^{-3}), and light levels moderate ($Q_p < 150$ MJ m^{-2} mo^{-1}).
396 Water availability does not immediately bring high rates of F_{GPP} indicating that the
397 ecosystem needs time to recover from summer drought stress and the forest ecosystem
398 remains a net carbon source.
399
400 (4) The transition back to winter conditions.
401
402 These features are highlighted in Figure 3. The timing of transition #2 (i.e., shift from a
403 continuous net daily carbon sink to a continuous net carbon source) had significant implications
404 on whether the old-growth stand was an annual net sink or source of carbon. In the 11 years of
405 data collection, the timing between the earliest and latest occurrence of maximum cumulative
406 CO_2 uptake (i.e., most negative ΣF_{NEE}) varied by 72 days and occurred as early as May 21 (2003)
407 and as late as August 1 (2006). The average occurrence of maximum cumulative net carbon
408 uptake was June 24 (transition #2 in Figure 3) and coincided with the end of the average rainy
409 season.

3.3 Interannual F_{NEE}, F_{GPP}, and F_{Reco} variability

Average annual F_{NEE} was -49 g C m^{-2} yr^{-1} ± 40 g C m^{-2} yr^{-1}, indicating that the forest was on average an annual net sink of carbon from 1998-2008. Interannual variability was high for annual F_{NEE} (on the order of 300 g C m^{-2} yr^{-1}) and resulted from variability in the larger component fluxes F_{GPP} and F_{Reco} (Figure 4). Annual F_{NEE} ranged from -217 (1999) to + 100 (2003) g C m^{-2} yr^{-1}, F_{GPP} from 1229 (2002) to 1635 (2003) g C m^{-2} yr^{-1}, and F_{Reco} from 1122 (2002) to 1735 (2003) g C m^{-2} yr^{-1}. Years with greater than average F_{Reco} included 1998, 2003, 2004, and 2006. Years with greater than average F_{GPP} included 2003, 2004, and 2006. Significant net carbon sink years (F_{NEE} > - 50 g C m^{-2} yr^{-1}) included 1999, 2002, 2006, 2007, and 2008. Strong sink years in 1999 and 2002 largely resulted from reduced respiration fluxes instead of increased F_{GPP}. Significant net carbon source years (F_{NEE} > + 50 g C m^{-2} yr^{-1}) included 1998 and 2003 and were driven by greater than normal respiration fluxes.

Annual anomalies in F_{Reco} and F_{GPP} were generally well correlated ($R^2 = 0.82$, $P < 0.001$) and each year was usually associated with either having both below normal or both above normal component fluxes (slope = + 0.72). Highest net annual carbon uptake in 1999 was caused by attenuated respiration driven by cooler and wetter than normal temperatures in the spring and relatively cool conditions in the summer, while wetter than normal spring conditions did not lead to a substantial increase in F_{GPP}. Moderate net annual carbon loss in 2003 was related to an increase in respiration rates driven by higher than normal temperatures in winter and spring and near-normal rainfall (i.e., there were no significant moisture limitations until the end of summer). Temperature anomalies in 2003 appeared to increase photosynthesis but at lower rates than respiration. Very low rates of F_{Reco} and F_{GPP} in 2002 were likely related to water stress during the summer, and possibly, from a delayed forest recovery after the very dry 2000-2001 year.

433 We found a significant ($P < 0.01$) relationship between annual F_{NEE} and the Composite
434 Climate Index as indicated in Figure 5. Strong positive (or warm) phases of the CCI (> +1) were
435 linked to near-neutral (2005) or moderate CO_2 source years (1998, 2003) while strong negative
436 (or cool) phases of the CCI (< -1) resulted in weak (2000), moderate (2008), and strong (1999)
437 carbon sink years. From 1999-2003, the climate indices transitioned to a more positive state
438 whilst annual carbon uptake at the old-growth forest declined on average and the stand was a
439 significant source of CO_2 in 2003. Since 2006, the climate indices have transitioned back
440 towards more negative phases and carbon uptake has increased over the last couple of years as
441 compared to 2003–2005.
442
443 **3.4 Interdecadal F_{NEP} and F_{ANPP} variability**
444 To extend the EC flux record and examine the role of multi-decadal climate variability on
445 stand carbon response, we present over 50 years of biometric, aboveground net primary
446 productivity at Wind River and modeled net CO_2 fluxes in Figure 6. Modeled fluxes were
447 calculated using the linear regression fit from Figure 5 which predicted annual CO_2 exchange
448 based on the annual CCI. Modeled (1952-1997) and measured (1998-2008) carbon fluxes are
449 presented here as net ecosystem production (F_{NEP}, where $+ F_{NEP} = - F_{NEE}$) so that positive F_{NEP}
450 represents a net carbon sink. This was done so that the carbon flux sign notation agreed with
451 F_{ANPP}. In Figure 6 we also illustrate key exogenous factors on stand carbon dynamics: the 6-
452 month SPI, a major Douglas-fir beetle infestation and tree kill in 1950-1951, a less severe but
453 significant beetle outbreak and tree kill in 1971, a major shift of the PDO in 1977, and smaller,
454 and less certain, PDO shifts in 1998 and 2003. From 1950-1977, the PDO was in a dominant
455 negative phase. These decades were associated with a mean positive SPI value of + 0.45 (i.e.,

456 wetter than normal conditions), and higher than average net carbon uptake (modeled mean F_{NEP}
457 = + 101.6 g C m^{-2} yr^{-1}) and aboveground net primary productivity (measured mean F_{ANPP} = 288 g
458 C m^{-2} yr^{-1}) (Figure 6). In contrast, the dominant positive PDO phase from 1977-1998 led to drier
459 than normal conditions (mean SPI = -0.20), and smaller net carbon uptake carbon fluxes (F_{NEP} =
460 + 24.9 g C m^{-2} yr^{-1}) and ANPP (mean measured F_{ANPP} = 238 g C m^{-2} yr^{-1}).

461 F_{ANPP} was in part difficult to interpret because it included tree mortality as well as carbon
462 assimilation for recruitment and growth. Maximum annual F_{ANPP} during the 1949-1952
463 remeasurement was likely due to the beetle tree kill in 1950-1951 and associated increases in
464 coarse woody debris. The second F_{ANPP} peak in 1971 was also likely due to increased tree
465 mortality and coarse woody debris from beetle infestation. Since no major disturbances have
466 occurred since, the later remeasurement periods likely indicate increased growth and recruitment
467 and reduced mortality during wetter than normal conditions, while decreased growth and
468 recruitment occurred during drier conditions. The F_{ANPP} trends are in rough agreement with the
469 modeled and measured F_{NEP} data (Figure 6).
470

471 **3.5 Mechanistic drivers and efficiency parameters**

472 In Figure 7, daily F_{NEE}, F_{GPP}, and F_{Reco} were segregated by season, annual climate phase,
473 and daily clear sky fraction to examine the effects of light conditions on ecosystem carbon
474 exchange. In general, maximum (most negative) spring and summer F_{NEE} occurred during
475 cloudy or partly cloudy conditions while maximum winter net uptake occurred on sunny or
476 partly cloudy days. Distinct CSF-flux differences were also observed by climate phase. Dark,
477 cloudy spring days were on average net carbon sources (0.3 g C m^{-2} day^{-1}) during positive CCI
478 years but net carbon sinks (-1.0 g C m^{-2} day^{-1}) in negative CCI years. Partly cloudy summer days

were net carbon sources (0.54 g C m^{-2} day^{-1}) during positive CCI years but net carbon sinks (-0.23 g C m^{-2} day^{-1}) during negative CCI years.

Sunny conditions led to higher average rates of both F_{GPP} (Δ = + 1.1 g C m^{-2} day^{-1}) and F_{Reco} (Δ = + 1.6 g C m^{-2} day^{-1}) during positive phase years as compared to sunny days in negative phase years. To tease out the mechanisms specifically controlling F_{GPP}, vapor pressure deficit, light use efficiency, and water use efficiency are plotted in Figure 8 as a function of CSF. Canopy conductance responses to CSF are plotted in Figure 9. Figure 8a shows a systematic increase in springtime δe as cloudiness decreases regardless of whether the year was in a positive, negative or neutral CCI phase, although positive CCI years had slightly lower (but insignificant) springtime δe values during all light environments. During the summer, in contrast, positive CCI years experienced on average higher δe (Δ = + 0.55 kPa) during partly cloudy and sunny days than during any other climate phase although no concurrent decrease in F_{GPP} is apparent in Figure 7e. It appears that a high atmospheric water demand did not lead to a significant reduction in photosynthesis during 2003 and 2005 summers.

Light use efficiency, in contrast to δe, increased with increasing cloudiness. LUE on average peaked during dark and cloudy (1.66 g C MJ^{-1}) and cloudy days (1.29 g C MJ^{-1}) (Figure 8b and 8e) illustrating the higher efficiency of the needleleaf canopy to utilize diffuse radiation for photosynthesis. Springtime LUE was higher during positive phase years (Figure 8e) and coincided with lower than average vapor pressure deficit levels (Figure 8a). In the summer, minimal differences in LUE were observed between climate phase years (8e) and the largest decline in LUE occurred between cloudy and partly cloudy skies. Water use efficiency, in a similar manner, also increased with cloudiness (Figure 8c and 8f). Positive climate years were more water use efficient than either neutral or negative climate years during the dry season.

Canopy conductance responses to clear sky fraction were distinct in both the spring and summer. Figure 9 shows mean afternoon G_c according to season and clear sky fraction (cloudy, partly cloudy, or sunny) for all flux measurement years. Maximum afternoon canopy conductance universally peaked during cloudy conditions (mean G_c = 8.23 mm s^{-1}) and declined as sky brightness increased (mean G_c = 3.80 mm s^{-1} during sunny conditions). Summertime G_c rates were slightly higher during cool phase years (G_c = 5.75 mm s^{-1}) than during either positive (G_c = 4.76 mm s^{-1}) or neutral (G_c = 5.19 mm s^{-1}) phase years. Significant deviations in G_c occurred in spring 1999 (ΔG_c = + 1.33 mm s^{-1}), spring 2003 (ΔG_c = + 1.93 mm s^{-1}), spring 2006 (ΔG_c = - 1.29 mm s^{-1}), and summer 2000 (ΔG_c = +1.00 mm s^{-1}). The largest anomalies in G_c were not correlated to precipitation-based drought (i.e., the 3-month SPI) although G_c was less than normal during the summer droughts of 2002 and 2003. Declined G_c rates in summer 2003 corresponded to higher than normal air temperatures and water vapor pressure deficits. G_c rates were more sensitive to shorter-term weather anomalies (e.g., cloudiness, air temperature) associated with dominant climate phase than precipitation.

4. Discussion

4.1 Old-growth carbon dynamics across multiple temporal scales

As successional endpoints, old-growth forests are predicted to be near carbon neutral (Odum 1965). Early studies suggested that as forests age, photosynthesis decreases while respiration continuous to increase (Kira & Shidei 1967). As such, it was hypothesized that any increase in net carbon uptake in old-growth stands implies a change to exogenous factors (e.g., climate, atmospheric CO_2 concentration) (Graumlich et al. 1989) as aboveground production in these ancient forests remains relatively constant after crown closure (Grier et al. 1981). Our

525 study sheds important insights into the magnitude and uncertainty of old-growth forests as net
526 carbon sinks as we presented over a decade of CO_2 exchange measurements under a full range of
527 climate conditions for a 500 year old forest with limited recent disturbance. This paper provides
528 the longest, continuous record of old-growth eddy flux exchange to date. To extend the time
529 series and look at multi-decadal climate variability on forest carbon response, we also presented
530 over 50 years of biometric measurements of growth, recruitment and mortality and 50 years of
531 modeled CO_2 flux exchange.

532 On average Wind River was a small annual net sink of carbon equaling 49 ± 40 g C m^{-2}
533 yr^{-1} from 1998-2008 (the eddy covariance record) and an estimated net sink of 65 g C m^{-2} yr^{-1}
534 from 1952-1997 (the modeled CO_2 flux record). Our EC estimates are in agreement with the
535 biometric estimates of Harmon et al. 2004 for Wind River (F_{NEP} = + 20 ± 130 g C m^{-2} yr^{-1}).
536 Between 1952 and 1997 a significant climate event occurred: the PDO switched from a dominant
537 negative phase to a dominant positive phase in mid-1977. The consequences of this phase shift
538 lasted for decades and were captured by our modeled carbon exchange (1952-1977 mean F_{NEE} =
539 - 101 g C m^{-2} yr^{-1}, 1977-1997 mean F_{NEE} = -25 g C m^{-2} yr^{-1}), F_{ANPP} measurements (1952-1977
540 mean = 288 g C m^{-2} yr^{-1}, 1977-1997 mean = 238 g C m^{-2} yr^{-1}), local climatological records
541 (1952-1977 mean SPI = +0.45, 1977-1997 mean SPI = -0.2), and Composite Climate Index
542 (1952-1977 mean CCI = -1.12, 1977-1997 mean CCI = +1.03). Our SPI record agrees with
543 findings by Mantua et al. (1997) and Mote et al. (2003) who showed that negative phases of the
544 PDO bring wetter than normal conditions while positive phases bring drier conditions to the
545 Pacific Northwest and by Wharton et al. (2009) who found a strong link between local Wind
546 River climatology and the three dominant Pacific Ocean oscillations. Our results strongly

547 suggest that Wind River is a stronger net carbon sink during negative climate years, coinciding
548 with wetter, cooler, and cloudier than normal conditions.

549 Low-elevation Douglas-fir stands in the western Cascade Mountains were once assumed
550 to be relatively insensitive to climate when compared to subalpine species, but Case & Peterson
551 2005 suggest that radial growth in low elevation Douglas-fir is limited by low summer
552 precipitation and high summer temperatures linked to positive PDO and warm ENSO events.
553 Furthermore, Graumlich et al. (1989) from tree ring analysis studied how variation in F_{ANPP} of
554 old-growth Douglas-fir forests from 1880-1979 is related to long-term trends in temperature and
555 precipitation. They found that F_{ANPP} was significantly correlated with summer temperatures at
556 lower frequencies (> 6 years) and significantly correlated with annual precipitation at higher
557 frequencies (< 3 years). Their results suggest that links between temperature and F_{ANPP} may be
558 driven by longer climate phases such as the PDO while precipitation and F_{ANPP} may be driven by
559 ENSO. Correlations between climate data and F_{ANPP} measurements at Wind River were difficult
560 to interpret because high F_{ANPP} in 1951 and 1971 appeared to be linked to the immediate effects
561 of beetle disturbance and associated increases in mortality and coarse woody debris. The decline
562 in F_{ANPP} ~five years later in 1958 and 1977 suggests that negative impacts of insect infestation
563 on stand carbon uptake were evident during these remeasurements. The timing of this lag
564 between insect disturbance and decreased F_{ANPP} agrees with other forest inventory observations
565 (e.g., Campbell et al. 2009, Pfeifer et al. 2010). Although it is common belief that beetle kill
566 events are higher during drought conditions because of increased tree stress, at Wind River
567 beetle kill events may be uncoupled from weather and instead are correlated with fungal
568 pathogens which thrive during wet events (K. Bible, personal communication). This could

explain why we observed higher F_{ANPP} in 1952 and 1971; a multi-decadal period of wetter conditions during the dominant negative PDO.

Our study showed a strong link between the SPI and CCI, between the SPI and modeled F_{NEE}, and a less certain link between the SPI and measured F_{ANPP} from 1952-1997 which suggests that teleconnection-induced variability in precipitation is a strong driver of net ecosystem exchange at Wind River. Small PDO switches likely occurred in mid-1998 (from positive to negative) and again in mid-2002 (from negative to positive). The 1998 PDO shift corresponded with a simultaneous strong ENSO phase change from El Niño to La Niña (warm to cool) in 1998-1999. Less significant, in-phase switches of the PNA were also observed in 2002. Coinciding with the 1998 PDO phase change, the old-growth forest was a strong carbon sink in 1999 (F_{NEE} = -217 g C m^{-2} yr^{-1}) as compared to the preceding carbon source year (F_{NEE} = +50 g C m^{-2} yr^{-1}). Carbon flux shifts were also observed between 2002 (F_{NEE} = -98 g C m^{-2} yr^{-1}) and 2003 (F_{NEE} = +100 g C m^{-2} yr^{-1}) corresponding to the negative to positive PDO shift.

El Niño-La Niña impacts on forest carbon exchange have been studied over a young-to-intermediate Douglas-fir stand (~60 years old) in coastal British Columbia (Morgenstern et al. 2004, Krishnan et al. 2009), a managed Ponderosa pine stand in the Sierra Nevada, California (Goldstein et al. 2000, Misson et al. 2005), and a mixed needleleaf forest in Howland, Maine (Zhang et al. 2011). In California, where El Niño brings cooler and wetter conditions than normal, maximum sink years occurred during El Niño events due to an increase in F_{GPP} from the wetter winter and spring months (Goldstein et al. 2000). In British Columbia, which has similar ENSO-related weather patterns as Wind River, Morgenstern et al. (2004) found that variance in annual F_{NEE} was linked to air temperature anomalies during the 1997–1999 period. During the

591 1997-1998 El Niño, they observed lower annual F_{NEE} (i.e., reduced net carbon uptake) in 1998
592 than during the following La Niña in 1999, likely due to higher F_{Reco} in 1998 than in 1999.
593 We noted a strong asymmetric pattern in peak F_{GPP} and F_{Reco} at Wind River. Maximum
594 photosynthesis normally occurred in May while maximum ecosystem respiration occurred two
595 months later in July-August. This 60-day lag between peak F_{GPP} and F_{Reco} is longer than
596 observed in other mid-latitude and younger forests. For example, Krishnan et al. (2009) report
597 less asymmetry in the 60 year old Douglas-fir stand in British Columbia and F_{GPP} and F_{Reco} both
598 peaked between July and August. Our strong asymmetry in the component fluxes is likely an
599 adaptive feature of old growth ecology and physiology to the strong seasonal climate whereby
600 F_{GPP} is optimized during the wetter, cloudier spring months and F_{Reco} follows a close trend with
601 temperature and peaks in the summer.
602
603 **4.2 Mechanistic drivers of CO_2 flux variability**
604 While trends in F_{NEE}, F_{GPP}, and R_{eco} appear to be linked to longer-scale teleconnection
605 patterns and perturbations in seasonal temperature and precipitation, the mechanisms which
606 control fluxes are also sensitive to environmental drivers across shorter-term scales. Numerous
607 studies have shown that tree canopy photosynthesis is more efficient under cloudy skies (e.g.,
608 Baldocchi 1997, Gu et al. 2002). Cloudy conditions are a common occurrence at Wind River
609 except during mid-summer and early autumn when a Pacific high pressure cell dominants the
610 region. We generally found higher rates of F_{GPP} on cloudy or partly cloudy days, likely because
611 of the associated changes in canopy light scattering, vapor pressure deficit, canopy temperature,
612 and water availability on photosynthesis. Clouds had a negative effect on daily F_{Reco} in late
613 spring, summer, and early autumn as the intensity and scattering of light affects how much

614 radiation hits the ground surface. This alters soil temperature and surface moisture, both of
615 which affect rates of heterotrophic and belowground autotrophic respiration. Cloudiness also
616 alters canopy albedo and leaf and bole temperatures affecting autotrophic respiration rates in the
617 canopy. Clouds had the effect of increasing net carbon uptake at Wind River except during very
618 dark and cloudy conditions which led to light limitations and substantially lower F_{GPP}.
619 In the tallest Douglas-fir trees at Wind River, the hydrological path length between the
620 roots and upper canopy stomata is greater than 50 m. This distance results in a decline in whole-
621 plant hydraulic conductance with height regardless of soil moisture (Ryan et al. 2000) which is
622 most attenuated on days with higher vapor pressure deficit (Waring & Franklin 1979). Lower G_c
623 rates restrict gas exchange (i.e., decreasing rates of transpiration and carbon assimilation) while
624 increasing leaf temperature and autotrophic respiration rates which result in a decrease in net
625 CO_2 uptake through lower light and water use efficiencies and higher autotrophic respiration
626 rates. We found that WUE was lowest on sunny days regardless of climate phase. This agrees
627 with other findings that WUE is a plastic characteristic for Douglas-fir trees and increases with
628 increasing light availability (Winner et al. 2004) and is inversely proportional to δe (Lindroth &
629 Cienciala 1996, Berbigier et al. 2001). LUE was also highest on cloudy days and suggests, in
630 lieu of diffuse radiation measurements, that the old-growth canopy is efficient at scattering
631 isotropic radiation.
632 We caution that a complete understanding of the mechanistic drivers of carbon exchange
633 is limited by the fact that most of the derived parameters used here (G_c, WUE, and LUE, and δe)
634 provide little insight into the drivers of ecosystem respiration and in particular, to the drivers of
635 heterotrophic versus autotrophic respiration. This is especially critical at Wind River
636 considering that total soil respiration scales from 67% to 79% of F_{Reco} (Falk et al. 2005).

637 Ongoing δC^{13} research at Wind River may provide additional clues to the importance of climate
638 variability on F_{NEE} as estimates of ecosystem respiration and its components can be derived via
639 isotopic signatures of the canopy boundary layer and background air (Keeling 1958).
640
641 **5. Conclusions**
642 The biometric and eddy covariance data presented here suggest that Wind River is not a
643 strong continuous sink of carbon as other recent EC and forest inventory studies have found in
644 mature and old-growth forest stands although on average it is a small net sink. This is in
645 agreement with recent modeling for old-growth stands done by Turner et al. 2011 and by the
646 biometric estimates at Wind River taken by Harmon et al. (2004). At Wind River the lack of
647 strong significant carbon sink activity may be attributable to the large amount of coarse woody
648 debris and subsequent large pool of potentially respiring carbon, and to restrictions on gas
649 exchange inhibiting photosynthesis in the upper canopy when atmospheric water demand is high
650 during the summer drought. We found that anomalies in annual F_{NEE} and to a lesser extent F_{ANPP}
651 were linked to climate perturbations driven by Pacific teleconnection events. Considering that
652 Pacific Northwest forests store more carbon per unit area than any other forest in North America
653 (Turner et al. 1995) and many climate models predict greatest future warming in the Pacific
654 Northwest to occur in the summer months with as much as a 20-40% decrease in summer
655 precipitation (Mote & Salathe 2010), our results suggest that any perturbations in climate
656 towards a warmer, drier state, such as would occur during dominant positive climate phases, will
657 have significant regional impacts on terrestrial carbon exchange and possibly global atmospheric
658 CO_2 concentration as respiration may increase without subsequent, offset increases in carbon
659 assimilation in these forests.

6. Acknowledgements

This research was supported by the Office of Science, US Department of Energy (Agreement No. DE-FC03-90ER61010). S.W. received additional funding through the Postdoctoral Research Program at the Lawrence Livermore National Laboratory. Lawrence Livermore National Laboratory is operated by Lawrence Livermore National Security, LLC, for the US Department of Energy, National Nuclear Security Administration under Contract DE-AC52-07NA27344. The Wind River Field Station operates from an agreement among the University of Washington, the Pacific Northwest Research Station (PNW), and the Gifford Pinchot National Forest.

669 **7. References**

670

671 Amiro, B.D., Barr, A.G., Black, T.A., Iwashita, H., Kljun, N., McCaughey, J.H., Morgenstern,
672 K., Murayama, S., Nesic, Z., Orchansky, A.L., Saigusa, N., 2006. Carbon, energy and water
673 fluxes at mature and disturbed forest sites, Saskatchewan, Canada. Agric. For. Meteorol. 136,
674 237-251.

675

676 Anthoni, P.M., Unsworth, M.H., Law, B.E., Irvine, J., Baldocchi, D.D., Van Tuyl, S., Moore, D.,
677 2002. Seasonal differences in carbon and water vapor exchange in young and old-growth
678 ponderosa pine ecosystems. Agric. For. Meteorol. 111, 203-222.

679

680 Arain, M.A., Restrepo-Coupe, N., 2005. Net ecosystem production in a temperate pine
681 plantation in southeastern Canada. Agric. For. Meteorol. 128, 223-241.

682

683 Aubinet, M., Chermanne, B., Vandenhaute, M., Longdoz, B., Yernaux, M., Laitat, E., 2001.
684 Long term carbon dioxide exchange above a mixed forest in the Belgian Ardennes. Agric. For.
685 Meteorol. 108, 293-315.

686

687 Baldocchi, D., 1997. Measuring and modelling carbon dioxide and water vapour over a
688 temperate broad-leaved forest during the 1995 summer drought. Plant Cell Environ. 20, 1108-
689 1122.

690

691 Baldocchi, D., 2008. "Breathing" of the terrestrial biosphere: lessons learned from a global
692 network of carbon dioxide flux measurement systems. Austral. J Bot. 56, 1-26.

693

694 Barr, A.G., Griffis, J., Black, T.A., Lee, X., Staebler, R.M., Fuentes, J.D., Chen, Z.,
695 Morgenstern, K., 2002. Comparing the carbon budgets of boreal and temperate deciduous forest
696 stands. Can. J. For. Res. 32, 813-822.

Barr, A.G., Black, T.A., Hogg, E.H., Griffis, T.J., Morgenstern, K., Kljun, N., Theede, A., Nesic, Z., 2007. Climatic controls on the carbon and water balances of a boreal aspen forest, Global Change Biol. 13, 561-576.

Berbigier, P., Bonnefond, J.-M., Mellmann, P., 2001. CO_2 and water vapour fluxes for 2 years above EuroFlux forest site. Agric. For. Meteorol. 108, 183–197.

Bergeron, O., Margolis, H.A., Black, T.A., Coursolle, C., Dunn, A.L., Barr, A.G., Wofsy, S.C., 2007. Comparison of carbon dioxide fluxes over three boreal black spruce forests in Canada. Global Change Biol. 13, 89-107.

Campbell, J., Alberti, G., Martin, J., Law, B.E., 2009. Carbon dynamics of a ponderosa pine plantation following a thinning treatment in the northern Sierra Nevada. For. Ecol. Manage. 257, 453-463.

Carrara, A., Kowalski, A.S., Neirynck, J., Janssens, I.A., Yuste, J.C., Ceulemans, R., 2003. Net ecosystem CO_2 exchange of mixed forest in Belgium over 5 years. Agric. For. Meteorol. 119, 209-227.

Case, M.J., Peterson, D.L., 2005. Fine-scale variability in growth-climate relationships of Douglas-fir, North Cascade Range, Washington. Can. J. For. Res. 35, 2743-2755.

Desai, A.R., Bolstad, P.V., Cook, B.D., Davis, K.J., Carey, E.V., 2005. Comparing net ecosystem exchange of carbon dioxide between an old-growth and mature forest in the upper Midwest, USA. Agric. For. Meteorol. 128, 35-55.

Dolman, A.J., Moors, E.J., Elbers, J.A., 2002. The carbon uptake of a mid latitude pine forest growing on sandy soil. Agric. For. Meteorol. 111, 157-170.

726 Dunn, A.L., Barford, C.C., Wofsy, S.C., Goulden, M.L., Daube, B.C., 2007. A long-term record
727 of carbon exchange in a boreal black spruce forest: means, responses to interannual variability,
728 and decadal trends. Global Change Biol. 13, 577-590.
729
730 Falk, M., Paw U, K.T., Wharton, S., Schroeder, M., 2005. Is soil respiration a major contributor
731 to the carbon budget within a Pacific Northwest old-growth forest? Agric. For. Meteorol. 135,
732 269-283.
733
734 Falk, M., Wharton, S., Schroeder, M., Ustin, S., Paw U, K.T., 2008. Flux partitioning in an old-
735 growth forest: seasonal and interannual dynamics. Tree Physiol. 28, 509-520.
736
737 Falge, E., Baldocchi D., Olson R., Anthoni, P., Aubinet, M., Bernhofer, C., Burba, G.,
738 Ceulemans, R., Clement, R., Dolman, H., Granier, A., Gross, P., Grunwald, T., Hollinger, D.,
739 Jensen, N.O., Katul, G., Keronen, P., Kowalski, A., Lai, C.T., Law, B.E., Meyers, T., Moncrieff,
740 H., Moors, E., Munger, J.W., Pilegaard, K., Rannik, U., Rebmann, C., Suyker, A., Tenhunen, J.,
741 Tu, K., Verma, S., Vesala, T., Wilson, K., Wofsy, S., 2001 Gap filling strategies for defensible
742 annual sums of net ecosystem exchange. Agric. For. Meteorol. 107, 43-69.
743
744 Franklin, J.F., Cromack, K., Denison, W., McKee, A., Maser, C., Sedell, J., Swanson, F., Juday,
745 G., 1981. Ecological Characteristics of Old-Growth Douglas-fir Forests, General Technical
746 Report PNW-118, Pacific Northwest Forest and Range Experiment Station, Portland, Oregon, 48
747 p.
748
749 Franklin, J.F., Spies, T.A., 1991. Ecological definitions of old-growth Douglas-fir forests, in:
750 Ruggiero, L.F., Aubry, K.B., Carey, A.B., Huff, M.H. (Eds.), Wildlife and Vegetation of
751 Unmanaged Douglas-fir Forests., U.S. Department of Agriculture, Forest Service, Portland,
752 Oregon, General Technical Report PNW-285.
753

754 Goulden, M.L., Munger, J.W., Fan, S.M., Daube, B.C., Wofsy, S.C., 1996. Exchange of carbon
755 dioxide by a deciduous forest: response to interannual climate variability. Science 271, 1576-
756 1578.
757
758 Graumlich, L.J., Brubaker, L.B., Grier, C.C., 1989. Long-term trends in forest net primary
759 productivity: Cascade Mountains, Washington. Ecology 70, 405-410.
760
761 Granier, A., Ceschia, E., Damesin, C., Dufrene, E., Epron, D., Gross, P., Lebaube, S., LeDantec,
762 V., Le Goff, N., Lemoine, D., Lucot, E., Ottorini, J.M., Pontailler, J.Y., Saugier, B., 2000. The
763 carbon balance of a young beech forest. Funct. Ecol. 14, 312–325.
764
765 Grier, C.C., Vogt, K.A., Keyes, M.R., Edmonds, R.L., 1981. Biomass distribution and above-
766 and belowground production in young and mature Abies amabalis zone ecosystems of the
767 Washington Cascades. Can. J. For. Res. 11, 155-167.
768
769 Griffis, T.J., Black, T.A., Morgenstern, K., Barr, A.G., Nesic, Z., Drewitt, G.B., Gaumont-Guay,
770 D., McCaughey, J.H., 2003. Ecophysiological controls on the carbon balances of three southern
771 boreal forests. Agric. For. Meteorol. 117: 53-71.
772
773 Grunwald, T., 2003. Langfristige Beobachtung von Kohlendioxidflussen mittels Eddy-
774 Kovarianz-Technik uber einem Altfichtenbestandim Tharandter Wald. Tharandter
775 Klimaprotokolle 7, 146 p.
776
777 Goldstein, A.H., Hultman, N.E., Fracheboud, J.M., Bauer, M.R., Panek, J.A., Xu, M., Qi, Y.,
778 Guenther, A.B., Baugh, W., 2000. Effects of climate variability on the carbon dioxide, water, and
779 sensible heat fluxes above a ponderosa pine plantation in the Sierra Nevada (CA). Agric. For.
780 Meteorol. 101, 113-129.
781

782 Gu, L., Baldocchi, D., Verma, S.B., Black, T.A., Vesala, T., Falge, E.M., Dowty, P.R., 2002.
783 Advantages of diffuse radiation for terrestrial ecosystem productivity. J Geophys. Res. 107(D6),
784 4050, doi:10.1029/2001JD001242.
785
786 Gusev, E.M., Nasonova, O.N., Dzhogan, L.Y., 2005. Modeling of heat-, water- and carbon-
787 exchange processes in a pine forest ecosystem. Atmos. Ocean. Phys. 41, 203-216.
788
789 Harmon, M.E., Bible, K., Ryan, M.G., Shaw, D.C., Chen, H., Klopatek, J., Li, X., 2004.
790 Production, respiration, and overall carbon balance in an old-growth Pseudotsuga-tsuga forest
791 ecosystem, Ecosystems 7, 498-512.
792
793 Hollinger, D.Y., Kelliher, F.M., Byers, J.N., Hunt, J.E., McSeveny, M., Weir, P.L., 1994. Carbon
794 dioxide exchange between an undisturbed old-growth temperate forest and the atmosphere.
795 Ecology 75, 134-150.
796
797 Hollinger, D.Y., Goltz, S.M., Davidson, E.A., Lee, J.T., Tu, K., Valentine, H.T., 1999. Seasonal
798 patterns and environmental control of carbon dioxide and water vapour exchange in an ecotonal
799 boreal forest. Global Change Biol. 5, 891-902
800
801 Hollinger, D.Y., Aber, J., Dail, B., Davidson, E.A., Goltz, S.M., Hughes, H., Leclerc, M.Y., Lee,
802 J.T., Richardson, A.D., Rodrigues, C., Scott, N.A., Achuatavarier, D., Walsh, J., 2004. Spatial
803 and temporal variability in forest-atmosphere CO_2 exchange. Global Change Biol. 10, 1689-
804 1706.
805
806 Hudiburg, T., Law, B., Turner, D.P, Campbell, J., Donato, D., Duane, M., 2009. Carbon
807 dynamics of Oregon and Northern California forests and potential land-based carbon storage.
808 Ecol. Appl. 19, 163-180.
809

Ishii, H., Reynolds J.H., Ford, E.D., Shaw, D.C., 2000. Height growth and vertical development of an old-growth Pseudotsuga–Tsuga forest in southwestern Washington State, USA. Can. J. For. Res. 30, 17–24.

Janssens, I.A., Lankreijer, H., Matteucci, G., Kowalski, A.S., Buchmann, N., Epron, D., Pilegaard, K., Kutsch, W., Longdoz, B., Grunwald, T., Montagnani, L., Dore, S., Rebmann, C., Moores, E.J., Grelle, A., Rannik, Ü., Morgenstern, K., Oltchev, S., Clement, R., Gudmundsson, J., Minerbi, S., Berbigier, P., Ibrom, A., Moncrieff, J., Aubinet, M., Bernhofer, C., Jensen, N.O., Vesala, T., Granier, A., Schulze, E.-D., Lindroth, A., Dolman, A.J., Jarvis, P.G., Ceulemans, R., Valentini, R., 2001. Productivity overshadows temperature in determining soil and ecosystem respiration across European forests. Global Change Biol. 7, 269–278.

Keeling, C.D., 1958. The concentrations and isotopic abundances of atmospheric carbon dioxide in rural areas. Geochimica et Cosmochimica Acta, 13, 322-334.

Kira T., Shidei, T., 1967. Primary production and turnover of organic matter in different forest ecosystems of the Western Pacific. Japan. J. Ecol. 17, 70-87.

Knohl, A., Schulze, E.-D., Kolle, O., Buchmann, N., 2003. Large carbon uptake by an unmanaged 250-year old deciduous forest in Central Germany. Agric. For. Meteorol. 118, 151-167.

Krishnan, P., Black, T.A., Jassal, R.S., Chen, b.Z., Nesic, Z., 2009. Interannual variability of the carbon balance of three different-aged Douglas-fir stands in the Pacific Northwest. J. Geophy. Res. – Biogeosci. 114, G04011, DOI: 10.1029/2008JG000912.

Lee, X.H., Fuentes, J.D., Staebler, R.H., Neumann, H.H., 1999. Long-term observation of the atmospheric exchange of CO_2 with a temperate deciduous forest in southern Ontario, Canada. J. Geophys. Res. - Atmos. 104, 15975-15984.

840 Leuning, R., Judd, M.J., 1996. The relative merits of open- and closed-path analysers for
841 measurement of eddy fluxes. Global Change Biol. 2, 241-253.
842
843 Lichstein, J.W., Wirth, C., Horn, H.S., Pacala, S.W., 2009. Biomass chronosequences of United
844 States forests: implications for carbon storage and forest management. *In:* Wirth, C., et al. (Eds.),
845 *Old-Growth Forests*. Springer-Verlag, Berlin.
846
847 Lindroth, A., Cienciala, E., 1996. Water use efficiency of short-rotation Salix viminalis at leaf,
848 tree and stand scales. Tree Physiol. 16, 257-262.
849
850 Lindroth, A., Grelle, A., Moren, A.S., 1998. Long-term measurements of boreal forest carbon
851 balance reveal large temperature sensitivity. Global Change Biol. 4, 443-450.
852
853 Loescher, H.W., Oberbauer, S.F., Gholz, H.L., Clark, D.B., 2003. Environmental controls on net
854 ecosystem-level carbon exchange and productivity in a Central American tropical wet forest.
855 Global Change Biol. 9, 396-412.
856
857 Luyssaert, S., Schulze, E.-D., Borner, A., Knohl, A., Hessenmoller, D., Law, B.E., Ciais, P.,
858 Grace, J., 2008. Old-growth forests as global carbon sinks. Nature 445, 213-215.
859
860 Ma, S., Baldocchi, D.D., Xu, L., Hehn, T., 2007. Inter-annual variability in carbon dioxide
861 exchange of an oak/grass savanna and open grassland in California. Agric. For. Meteorol. 147,
862 157-171.
863
864 Madden, R.A., Julian, P.R., 1971. Detection of a 40-50 day oscillation in the zonal wind in the
865 tropical Pacific. J. Atmos Sci. 28, 702-708.
866
867 Mantua, NJ, Hare, SR, Zhang, Y, Wallace, JM, Francis, RC, 1997. A Pacific interdecadal
868 climate oscillation with impacts on salmon production. Bull. Amer. Meteorol. Soc. 78, 1069-
869 1079.

870 Mantua, N.J., Hare, S.R., 2002. The Pacific Decadal Oscillation, J. Oceanogr. 58, 35-44.
871
872 Markkanen, T., Rannik, U., Keronen, P., Suni, T., Vesala, T., 2001. Eddy covariance fluxes over
873 a boreal Scots pine forest, Boreal Environ. Res. 6, 65-78.
874
875 Massman, W.J., Lee, X., 2002. Eddy covariance flux corrections and uncertainties in long-term
876 studies of carbon and energy exchanges. Agric. For. Meteorol. 113, 121–144.
877
878 McKee, T.B., Doesken, N.J., Kleist, J., 1993. The relationship of drought frequency and duration
879 to time scales. Eighth Conf. Appl. Climatol., Anaheim, California, USA, 179–184.
880
881 Misson, L, Tang, J., Xu, M., McKay, M., Goldstein, A., 2005. Influences of recovery from clear-
882 cut, climate variability, and thinning on the carbon balance of a young ponderosa pine plantation.
883 Agric. For. Meteorol. 130, 207-222.
884
885 Monteith, J.L., 1964. Evaporation and environment. In The State and Movement of Water in
886 Living Organisms. 19th Symposium of the Society on Experimental Biology. Academic Press,
887 New York, 205 p.
888 Monteith, J.L., 1972. Solar radiation and production in tropical ecosystems. J. Appl. Ecol. 9,
889 747–766.
890
891 Monteith, J.L., 1977. Climate and the efficiency of crop production in Britain. Philos. Trans. R.
892 Soc. London, Ser. B 281, 277–294.
893
894 Moore, C.J., 1986. Frequency response corrections for eddy covariance systems. Boundary
895 Layer Meteorol. 37, 17-35.
896
897 Morgenstern, K., Black, T.A., Humphreys, E.R., Griffis, T.J., Drewitt, G.B., Cai, T., Nesic, Z.,
898 Spittlehouse, D.L., Livingston, N.J., 2004. Sensitivity and uncertainty of the carbon balance of a

899 Pacific Northwest Douglas-fir forest during an El Niño/La Niña cycle. Agric. For. Meteorol.
900 123, 201-219.
901
902 Mote, P.W., Parson, E., Hamlet, A.F., Keeton, W.S., Lettenmaier, D., Mantua, N., Miles, E.L.,
903 Peterson, D., Peterson, D.L., Slaughter, R., Snover, A.K., 2003. Preparing for climatic change:
904 the water, salmon, and forests of the Pacific Northwest. Clim. Change 61, 45–88.
905
906 Mote, P.W., Salathe, E.P., 2010. Future climate in the Pacific Northwest. Clim. Change 102, 29-
907 50.
908
909 Odum, E., 1965. Fundamentals of Ecology. Saunders, Philadelphia, USA.
910
911 Parker, G.G., Davis, M.M., Chapotin, S.M., 2002. Canopy light transmittance in Douglas-fir-
912 western-hemlock stands. Tree Physiol. 22, 147–157.
913
914 Pfeifer, E.M., Hicke, J.A., Meddens, A.J.H., 2010. Observations and modeling of aboveground
915 tree carbon stocks and fluxes following a bark beetle outbreak in the western United States.
916 Global Change Biol. 17, 339-350.
917
918 Rasmusson, E.M., Wallace, J.M., 1983. Meteorological aspects of El Nino/Southern Oscillation,
919 Science 222, 1195-1202.
920
921 Reichstein, M., Tenhunen, O., Roupsard, J., Ourcival, M., Rambal, S., Miglietta, F., Peressotti,
922 A., Pecchiari, M., Tirone, G., Valentini, R., 2003. Inverse modeling of seasonal drought effects
923 on canopy CO_2/H_20 in three Mediterranean ecosystems. . J. Geophys. Res. - Atmos. 108, D23,
924 doi: 10.1029/2003JD003430.
925
926 Reichstein, M., Falge, E., Baldocchi, D., Papale, D., Aubinet, M., Berbigier, P., Bernhofer,
927 C., Buchmann, N., Gilmanov, T., Granier, A., Grunwald, T., Havrankova, K., Ilvesniemi, H.,
928 Janous, D., Knohl, A., Laurila, T., Lohila, A., Loustau, D., Matteucci, G., Meyers, T., Miglietta,

F., Ourcival, J.-M., Pumpanen, J., Rambal, S., Rotenberg E., Sanz, M., Tenhunen, J., Seufert, G., Vaccari, F., Vesala, T., Yakir, D., Valentini, R., 2005. On the separation of net ecosystem exchange into assimilation and ecosystem respiration: review and improved algorithm. Global Change Biol. 11, 1424–1439.

Richardson, A.D., Hollinger, D.Y., Aber, J.D., Ollinger, S.V., Braswell, B.H., 2007. Environmental variation is directly responsible for short- but not long-term variation in forest-atmosphere carbon exchange. Global Change Biol. 13, 788-803.

Roberts, D.A., Ustin, S.L., Ogunjemiyo, S., Greenberg, J., Dobrowski, S.Z., Chen, J., Hinckley, T.M., 2004. Spectral and structural measures of Northwest forest vegetation at leaf to landscape scales. Ecosystems 7, 545-562.

Rocha, A.V., Goulden, M.L., Dunn, A.L., Wofsy, S.C., 2006. On linking interannual tree ring variability with observations of whole-forest CO_2 flux. Global Change Biol. 12, 1378-1389.

Rosenberg, N.J., Blad, B.L., Verma, S.B., 1983. Microclimate, The Biological Environment, 2nd edn. John Wiley & Sons, New York, 495 p.

Saigusa, N., Yamamoto, S., Murayama, S., Kondo, H., Nishimura N., 2002. Gross primary production and net ecosystem exchange of a cool- temperate deciduous forest estimated by the eddy covariance method. Agric. For. Meteorol. 112, 203-215.

Schotanus, P., Nieuwstadt, F., DeBruin, H., 1983. Temperature-measurement with a sonic anemometer and its application to heat and moisture fluxes. Boundary-Layer Meteorol. 26, 81-93.

Shaw, D.C., Franklin, J.F., Bible, K., Klopatek, J., Freeman, E., Greene, S., Parker, G.G., 2004. Ecological setting of the Wind River old-growth forest. Ecosystems 7, 427-439.

959 Stewart, J.B., 1988. Modelling surface conductance of pine forests. Agric. For. Meteorol. 43, 19-
960 35.
961
962 Tan, Z.H., Zhang, Y.P., Schaefer, D., Yu, G.R., Liang, N.S., Song, Q.H., 2011. An old-growth
963 subtropical Asian evergreen forest as a large carbon sink. Atmos. Environ. 45, 1548-1554.
964
965 Thomas, S.C., Winner, W.E., 2000. Leaf area index of an old-growth Douglas-fir forest
966 estimated from direct structural measurements in the canopy. Can J. For. Res. 30, 1922–1930.
967
968 Thornton P.E., Law, B.E., Gholz, H.L., Clark, K.L., Falge, E., Ellsworth, D.S., Goldstein, A.H.,
969 Monson, R.K., Hollinger, D., Falk, M., Chen, J., Sparks, J.P., 2002. Modeling and measuring the
970 effects of disturbance history and climate on carbon and water budgets in evergreen needleleaf
971 forests. Agric. For. Meteorol. 113, 185–222.
972
973 Turner, D.P., Koerper, G.J., Harmon, M.E., Lee, J.J., 1995. A carbon budget for forests of the
974 conterminous United States. Ecol. Appl. 5, 421-436.
975
976 Turner, D.P., Ritts, W.D., Yang, Z.-Q., Kennedy, R.E., Cohen, W.B., Duane, M.V., Thornton,
977 P.E., Law, B.E., 2011. For. Ecol. Man. 262, 1318-1325.
978 Unsworth, M.H., Phillips, N., Link, T., Bond, B.J., Falk, M., Harmon, M.E., Hinckley, T.M.,
979 Marks, D., Paw U, K.T., 2004. Components and controls of water flux in an old-growth
980 Douglas-fir-western hemlock ecosystem. Ecosystems 7, 468-481.
981
982 Urbanski, S., Barford, C., Wofsy, S., Kucharik, C., Pyle, E., Budney, J., McKain, K., Fitzjarrald,
983 D., Czikowsky, M., Munger, J.W., 2007. Factors controlling CO_2 exchange on timescales from
984 hourly to decadal at Harvard forest. J. Geophys. Res. 112, G02020, doi:10.1029/2006JG000293.
985
986 Valentini, R., Matteucci, G., Dolman, A.J., Schulze, E.-D., Rebmann, C., Moors, E.J., Granier,
987 A., Gross, P., Jensen, N.O., Pilegaard, K., Lindroth, A., Grelle, A., Bernhofer, C., Grunwald, T.,
988 Aubinet, M., Ceulemans, R., Kowalski, A.S., Vesala, T., Rannik, Ü., Berbigier, P., Loustau, D.,

Gudmundsson, J., Thorgeirsson, H., Ibrom, A., Morgenstern, K., Clement, R., Moncrieff, J., Montagnani, L., Minerbi, S., Jarvis, P., 2000. Respiration as the main determinant of carbon balance in European forests. Nature 404, 861–865.

Wallace, J.M., Gutzler, D.S., 1981. Teleconnections in the geopotential height field during the Northern Hemisphere winter. Mon. Weath. Rev. 109, 784-812.

Waring, R.H., Franklin, J.F., 1979. Evergreen coniferous forests of the Pacific Northwest. Science 204, 1380-1386.

Wharton, S., Chasmer, L., Falk, M., Paw U, K.T., 2009. Strong links between teleconnections and ecosystem exchange found at a Pacific Northwest old-growth forest from flux tower and MODIS EVI data. Global Change Biol. 15, 2187-2205.

Wilson, J.D., Swaters, G.E., 1991. The source area influencing a measurement in the planetary boundary-layer – the footprint and the distribution of contact distance. Boundary-Layer Meteor. 55, 25-46.

Winner, W.E., Thomas, S.C., Berry, J.A., Bond, B.J., Cooper, C.E., Hinckley, T.M., Ehleringer, J.R., Fessenden, J.E., Lamb, B., McCarthy, S., McDowell, N.G., Phillips, N,., Williams, M., 2004. Canopy carbon gain and water use: analysis of old-growth conifers in the Pacific Northwest. Ecosystems 7, 482-497.

Zhang, J.Y., Wu, L.Y., Huang, G., Notaro, M., 2011. Relationships between large-scale circulation patterns and carbon dioxide exchange by a deciduous forest. J. Geophys. Res. – Atmos. 116, D04102, DOI: 10.1029/2010JD014738.

1017 Tables

1018

	Negative CCI years	Positive CCI years	Neutral CCI years	Historical mean
Annual T_{air} (°C)	8.5	9.3	9.1	8.8
Dry season T_{air} (°C)	14.5	15.6	15.3	14.8
Peak growing season T_{air} (°C)	8.8	10.2	9.9	9.7
Water-year P (mm)	2463	1855	2077	2338
Dry season P (mm)	206	242	233	322
Peak growing season P (mm)	437	550	462	567

1019 Table 1: Mean annual and seasonal air temperature and precipitation associated with the
1020 composite climate index (CCI) during flux measurement years (1998-2009) as well as the
1021 historical (1919-1997) mean. Positive CCI years are generally warmer and drier than average
1022 while negative CCI years are cooler and wetter. Water-year is November-October, peak growing
1023 season is March-June, and dry season is July-October.

1024

1025

1026

1027

1028

1029

1030

1031

1032

1033

	Peak F_{NEE} sink month	Peak F_{GPP} month	Peak F_{Reco} month	Annual F_{NEE} (g C m^{-2} yr^{-1})	CCI
1998*	April	May	August	+ 50	+
1999	April	August	August	- 217	-
2000	May	May	August	- 43	-
2001	April	May	July	- 30	neutral
2002	April	May	July	- 98	neutral
2003	April	June	July	+ 100	+
2004	May	May	July	- 9	neutral
2005*	May	May	July	+ 13	+
2006	April	July	July	- 114	neutral
2007	April	May	July	- 67	neutral
2008	April	May	August	- 111	-

1034 Table 2: Timing of maximum monthly net ecosystem exchange, gross primary productivity, and
1035 ecosystem respiration in comparison to annual F_{NEE} and CCI. Note that 1998 and 2005 were
1036 partially gap-filled using Biome-BGC because of high amounts of missing data.

1037

1038

1039

1040

Figure Headings

Figure 1: Seasonal total precipitation (top panel) and mean air temperature (bottom panel) for each of the flux measurements years as well as the historical mean and annual Composite Climate Index (CCI) phase. Precipitation is based on the water-year. Important climate anomalies included: cold winters in 2001 and 2004, a warm winter in 2003, a cold spring 2008, a warm summer 2003, dry summers in 2002 and 2006, a wet summer 2004, a dry spring 2007, dry winters in 2001 and 2005, and a wet winter 1999.

Figure 2: Time series of (a) monthly CCI, (b) running 6-month SPI, (c) running 3-month SPI, and monthly precipitation for all flux years. The SPI is based on the 1919-2008 precipitation record. Gray panels show 3-month drought events in winter 2001, summer/autumn 2002, autumn 2003, winter 2005, and spring 2007. Positive CCI values are generally linked to drier than normal precipitation conditions and negative SPI while negative CCI values are generally linked to above normal precipitation and positive SPI.

Figure 3: Average (a) daily F_{GPP} and F_{Reco} and (b) cumulative daily F_{NEE} and monthly mean Q_p and δ_e during neutral climate years show a typical asymmetric pattern in the timing of peak F_{GPP}, F_{Reco}, and F_{NEE}. This asymmetry is likely driven by relatively high light levels in spring and low vapor pressure deficit which leads to peak rates of F_{GPP} and moderate F_{Reco}, resulting in maximum net carbon uptake.

Figure 4: A decade of annual (a) F_{Reco}, (b) F_{GPP}, and (c) F_{NEE} estimates at Wind River show high interannual variability. The old-growth forest has switched from a moderate net sink of carbon (1999) to a moderate net source (2003) coinciding with a climate phase shift from positive to negative. The dotted lines represent the long-term mean.

Figure 5: Annual F_{NEE} (1998-2008) as a function of the CCI shows that net carbon sink years are generally associated with more negative (cool) climate phases while net carbon source years are associated with strongly positive (warm) climate phases. Data are fit with a linear regression line (Pearson's r value = 0.78, $P < 0.005$, y-intercept = -57 g C m^{-2} yr^{-1}).

Figure 6: Time series of (a) running 3-month SPI and (b) modeled F_{NEP} (1952-1997) based on the CCI, measured EC F_{NEP} (1998-2008), and measured biometric F_{ANPP} (1952-2004). + F_{NEP} = - F_{NEE}, so that positive F_{NEP} represents a net carbon sink year. Arrows represent significant external events including a large Douglas-fir beetle tree kill in 1951, a smaller but significant beetle tree kill in 1971, a major PDO switch (cool to warm) in 1977, and less certain and smaller PDO switches in 1998 and 2003. The SPI data show wetter conditions (positive values) than average from 1952-1977, coinciding with higher net carbon uptake in the modeled F_{NEP} series. As the climate state has become drier over the last 30 years it also appears that F_{ANPP} has decreased following the SPI and modeled F_{NEP} trend.

Figure 7: Mean daily F_{NEE}, F_{GPP}, and F_{Reco} by season, climate phase and clear sky fraction (CSF). Maximum carbon uptake occurred on spring-time cloudy or partly cloudy days during negative

climate phase years. This was driven by a combination of higher rates of F_{GPP} and attenuated F_{Reco}.

Figure 8: Seasonal mean daily maximum vapor pressure deficit, midday light use efficiency and midday water use efficiency as a function of CSF during negative, positive, and neutral phase years. Sunny days led to significantly higher δe, lower LUE, and slightly lower WUE during all light levels and seasons, while δe, WUE and LUE were generally lower during negative climate phases regardless of light conditions or season.

Figure 9: Mean afternoon canopy conductance rates (G_c) by CSF in (a) spring and (b) summer with the annual climate phase indicated. Dotted lines are the 1999-2008 mean, **** represent annual mean. Year to year as well as light-related differences are apparent and G_c rates on average are lower than the long-term mean during drought events based on the 3-month SPI. The highest G_c rates are observed in 1999 and 2003 in spring and in 2000 in summer and correspond to non-drought conditions.

1 Figures

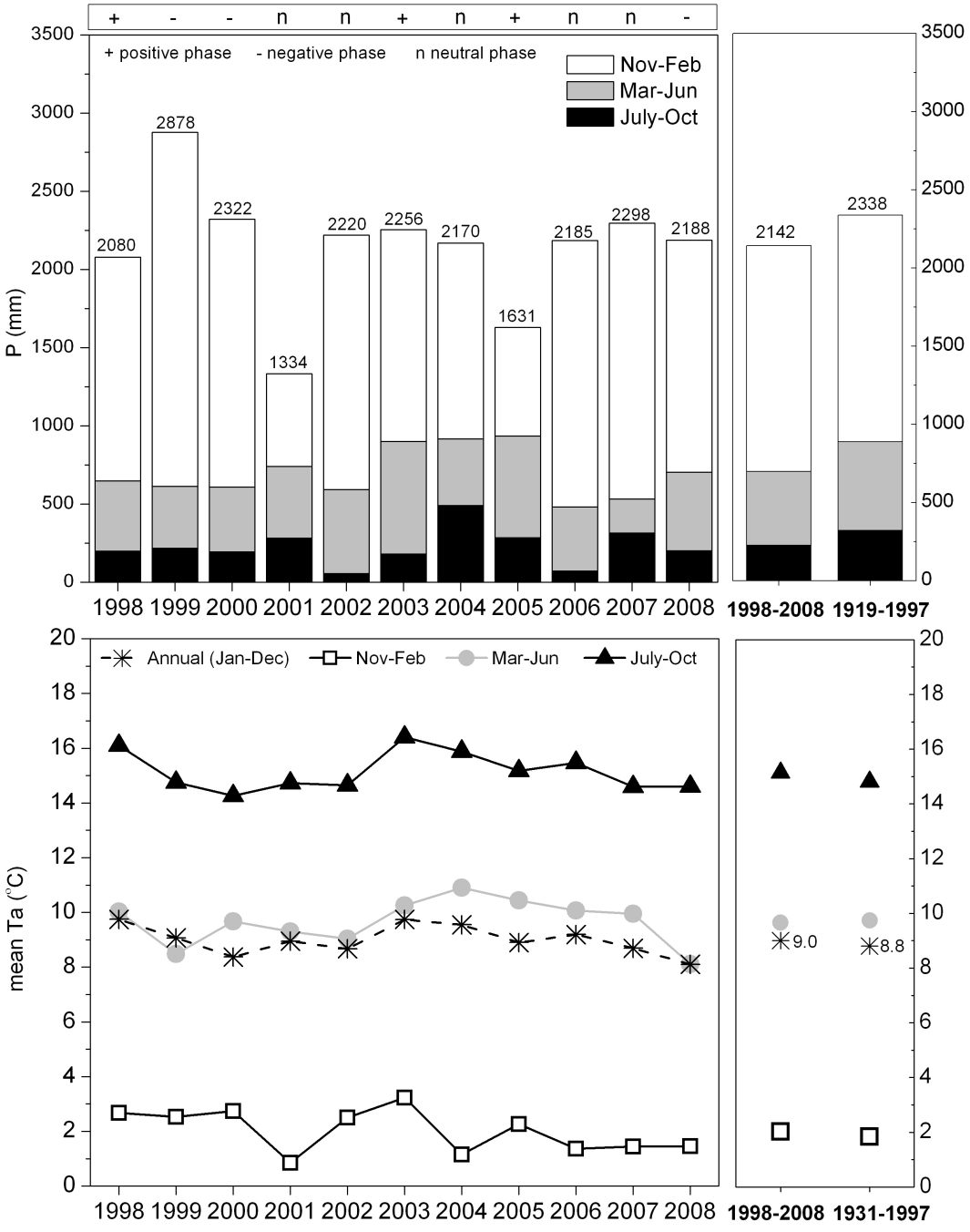

2

3 Figure 1

4

1

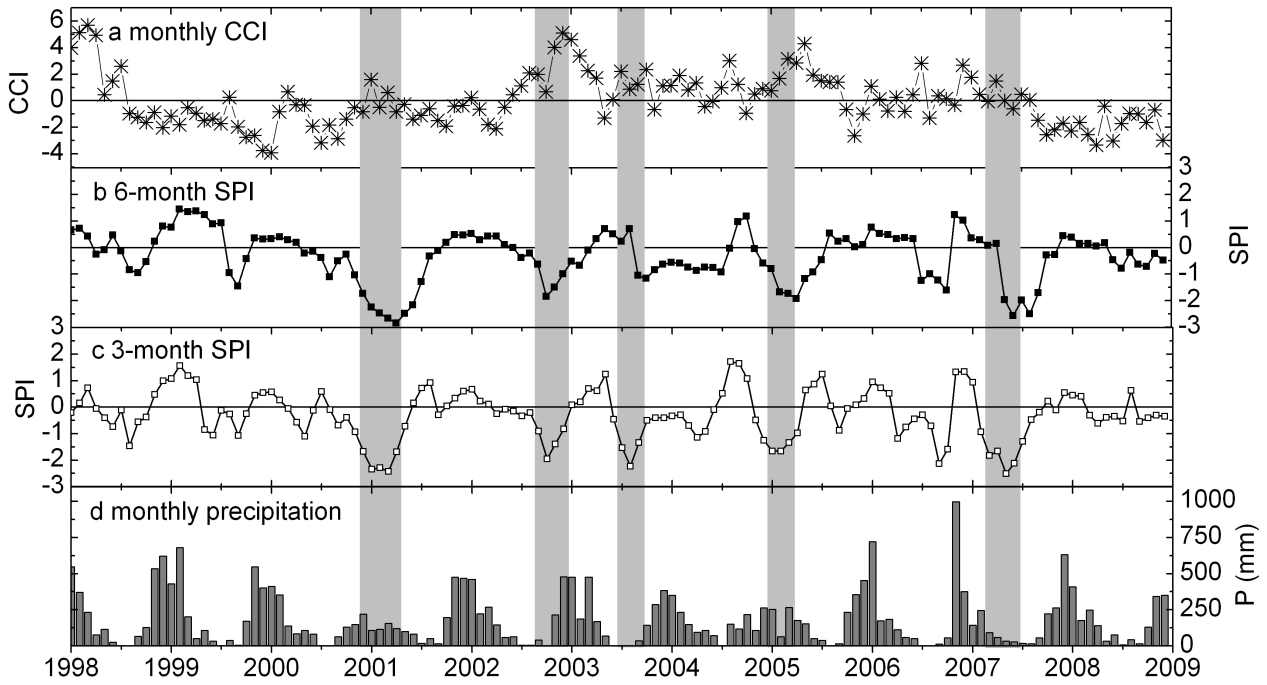

2

3 Figure 2

4

5

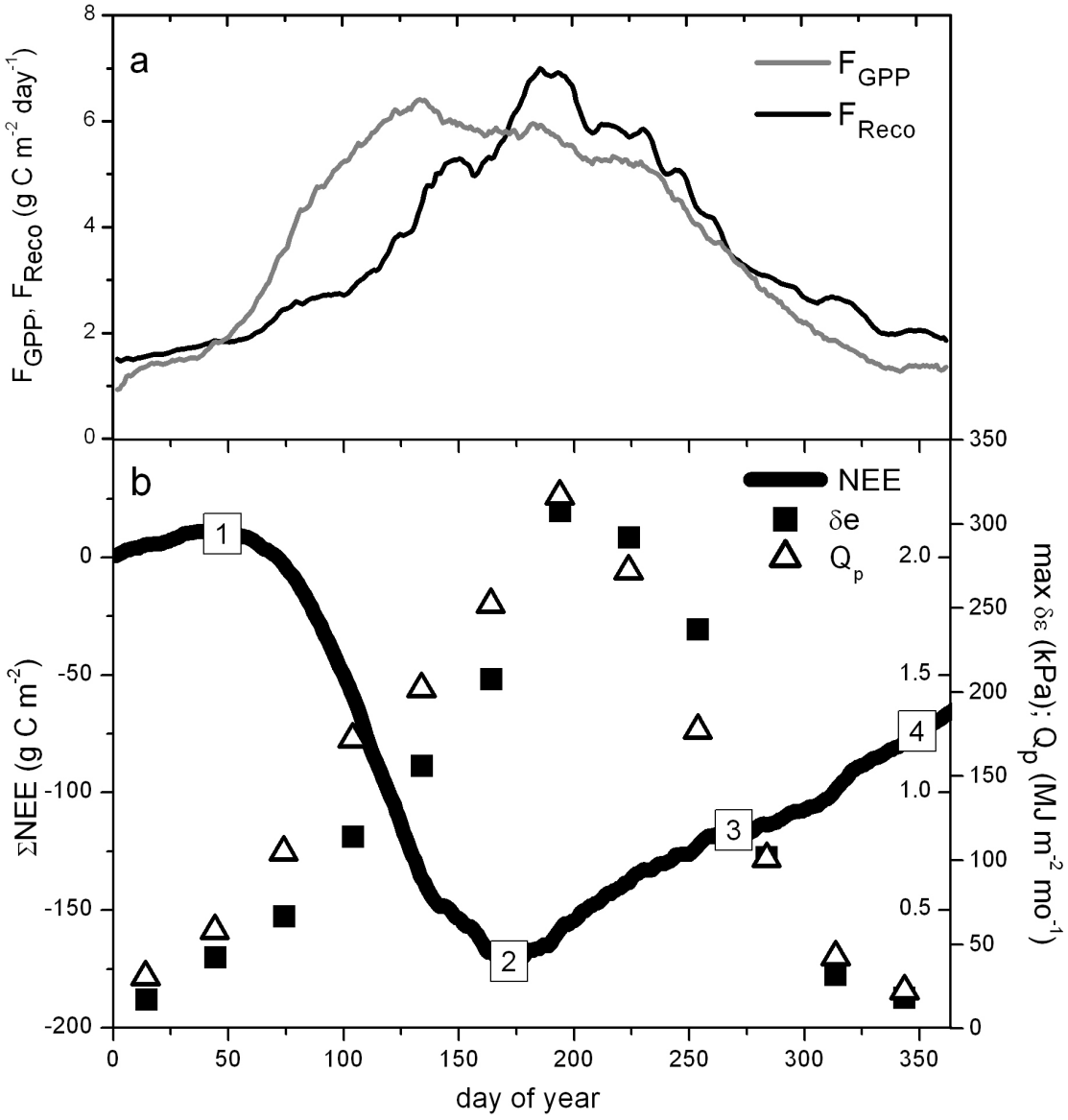

1

2 Figure 3

3

4

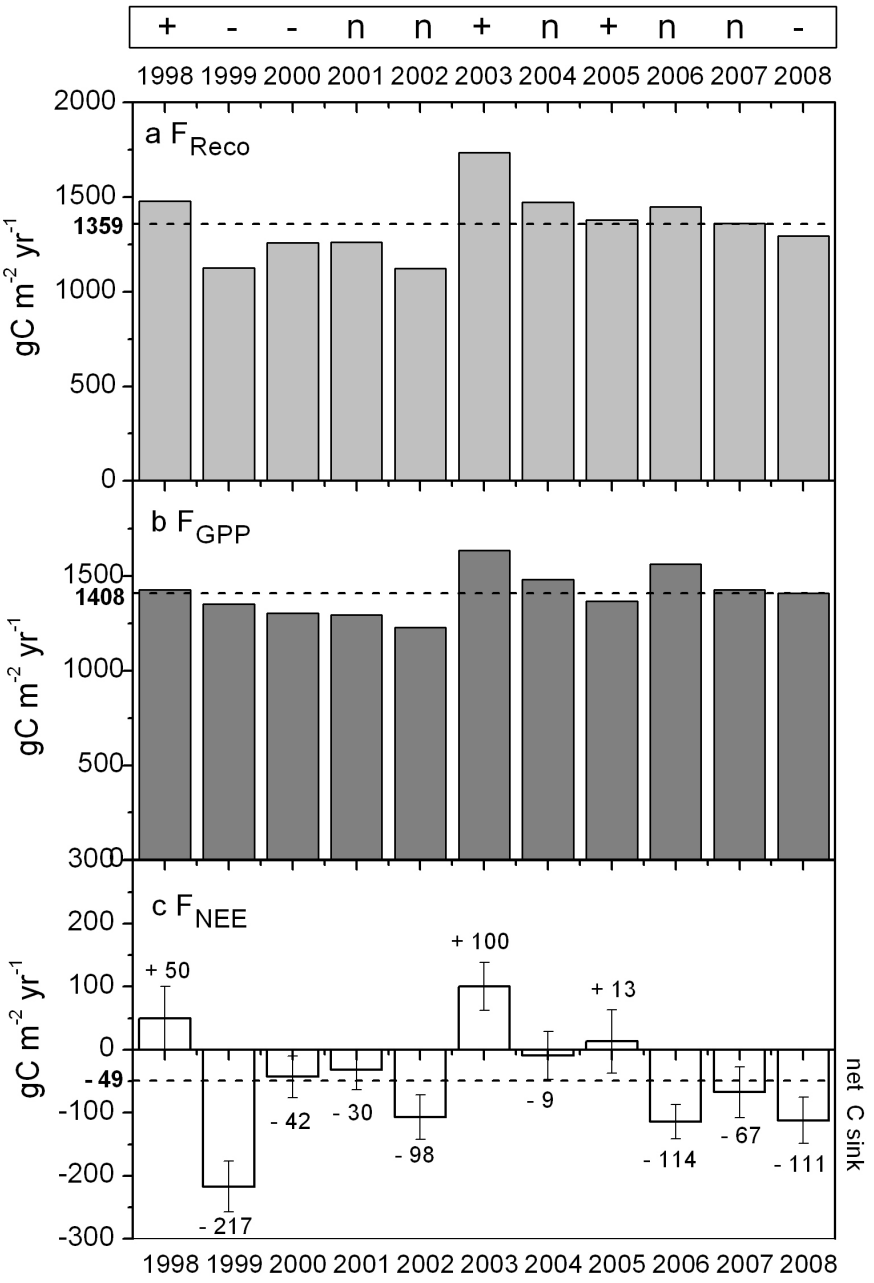

1

2 Figure 4

3

4

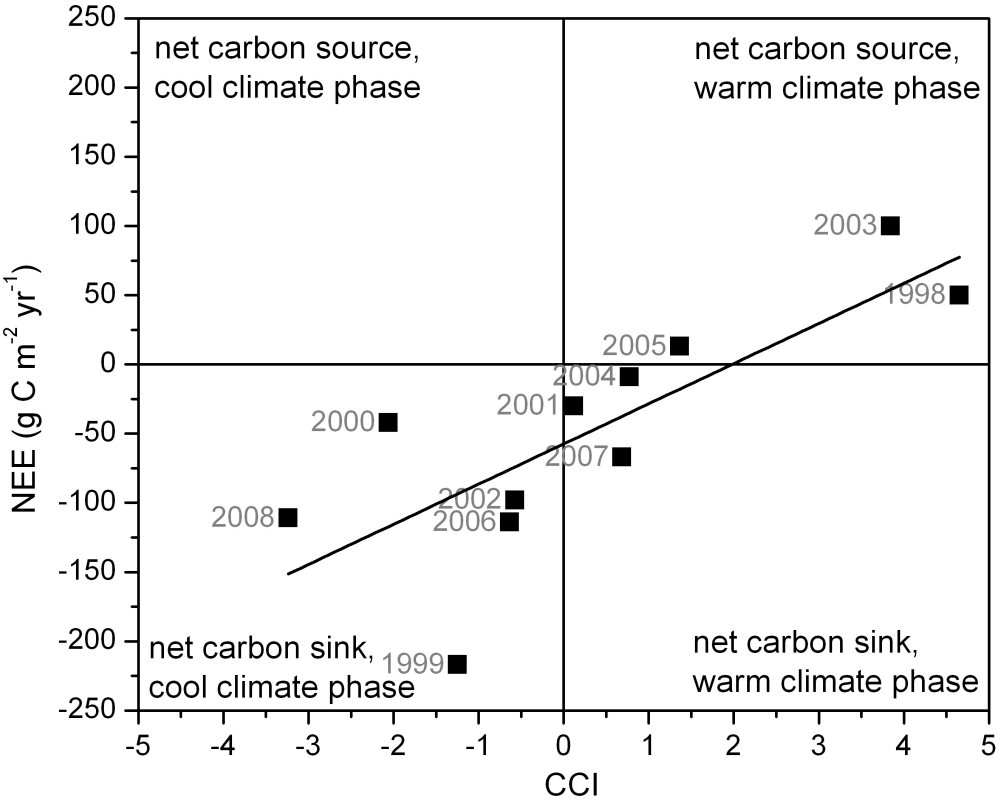
net carbon source,
cool climate phase
net carbon source,
warm climate phase
net carbon sink,
cool climate phase
net carbon sink,
warm climate phase
2003
1998
2005
2004
2001
2000
2007
2002
2006
2008
1999
NEE (g C m-2 yr-1)
CCI
250
200
150
100
50
0
-50
-100
-150
-200
-250
-5
-4
-3
-2
-1
0
1
2
3
4
5

Figure 5

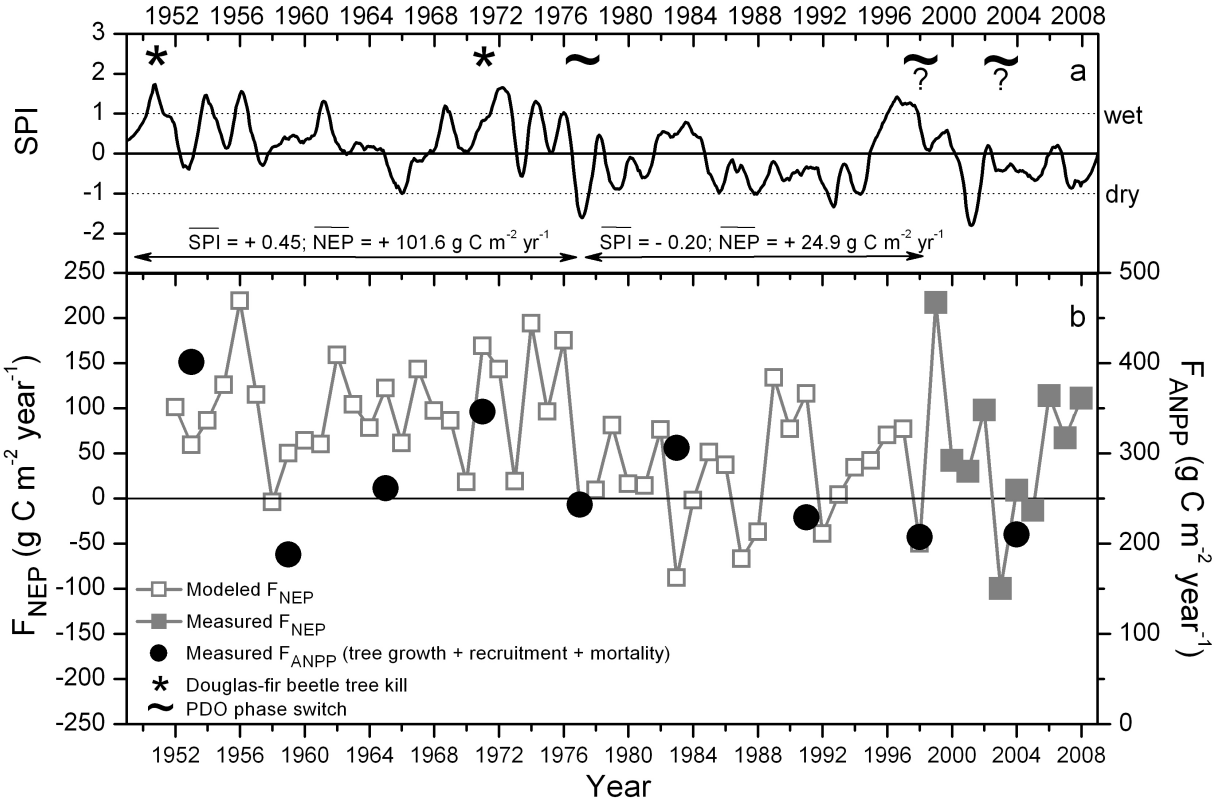
1952 1956 1960 1964 1968 1972 1976 1980 1984 1988 1992 1996 2000 2004 2008
SPI
a
wet
dry
SPI = + 0.45; NEP = + 101.6 g C m-2 yr-1
SPI = - 0.20; NEP = + 24.9 g C m-2 yr-1
b
FNEP (g C m-2 year-1)
FANPP (g C m-2 year-1)
Modeled FNEP
Measured FNEP
Measured FANPP (tree growth + recruitment + mortality)
Douglas-fir beetle tree kill
PDO phase switch
Year

1

2 Figure 6

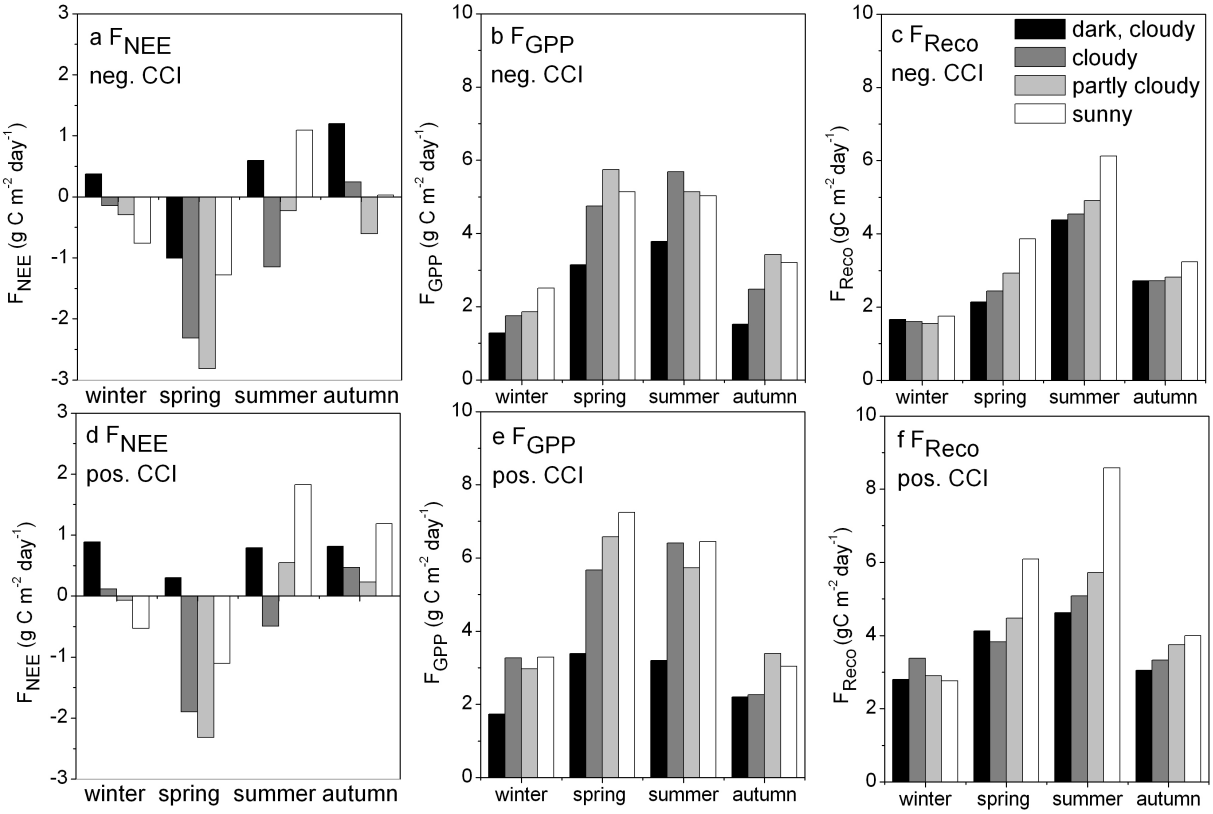
a F_{NEE}
neg. CCI
b F_{GPP}
neg. CCI
c F_{Reco}
neg. CCI
dark, cloudy
cloudy
partly cloudy
sunny
d F_{NEE}
pos. CCI
e F_{GPP}
pos. CCI
f F_{Reco}
pos. CCI
F_{NEE} (g C m^{-2} day^{-1})
F_{GPP} (g C m^{-2} day^{-1})
F_{Reco} (gC m^{-2} day^{-1})
winter
spring
summer
autumn

1

2 Figure 7

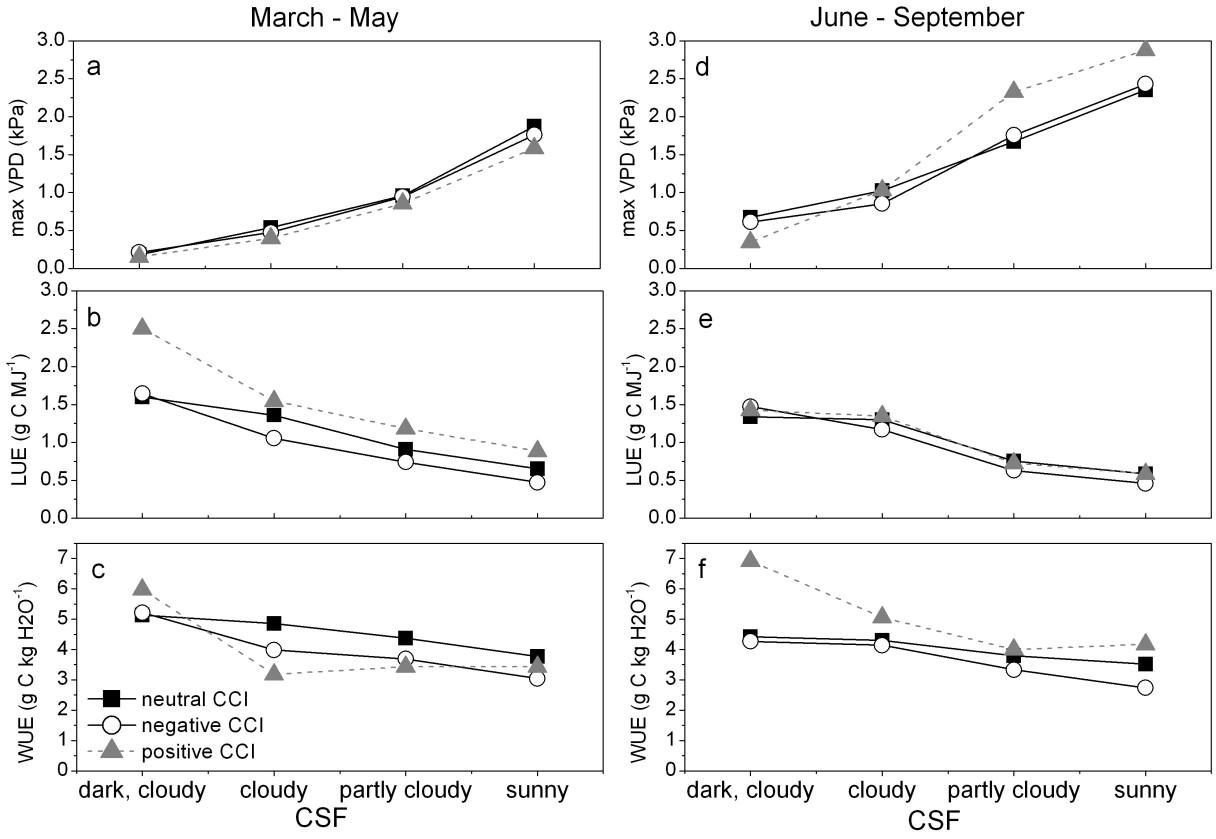
March - May
June - September
a
b
c
d
e
f
max VPD (kPa)
LUE (g C MJ-1)
WUE (g C kg H2O-1)
neutral CCI
negative CCI
positive CCI
dark, cloudy
cloudy
partly cloudy
sunny
CSF

Figure 8

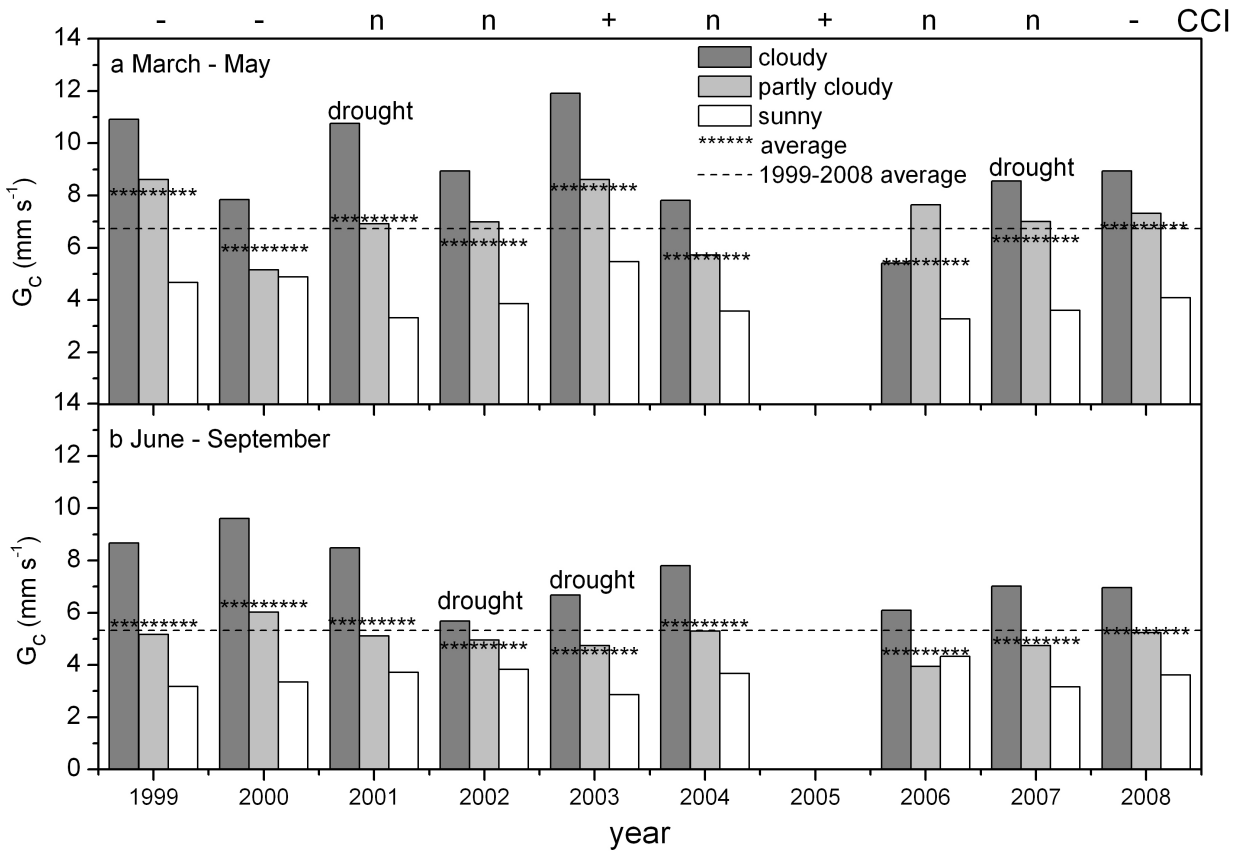
- - n n + n + n n - CCI
a March - May
b June - September
cloudy
partly cloudy
sunny
****** average
----- 1999-2008 average
drought
G_C (mm s^{-1})
year
1999
2000
2001
2002
2003
2004
2005
2006
2007
2008

Figure 9